A&A 466, 255–259 (2007)
DOI: 10.1051/0004-6361:20066955

Astronomy & Astrophysics

Isotopic ethyl cyanide $^{13}CH_3CH_2CN$, $CH_3{}^{13}CH_2CN$, and $CH_3CH_2{}^{13}CN$: laboratory rotational spectrum and detection in Orion⋆,⋆⋆

K. Demyk[1], H. Mäder[2], B. Tercero[3], J. Cernicharo[3], J. Demaison[1], L. Margulès[1], M. Wegner[2], S. Keipert[2], and M. Sheng[2]

[1] Laboratoire de Physique des Lasers, Atomes et Molécules, UMR CNRS 8523, Université Lille 1, 59655 Villeneuve d'Ascq Cedex, France
e-mail: Karine.demyk@univ-lille1.fr
[2] Universität Kiel, Institut fuer Physikalische Chemie Olshausenstrasse 40, 24098 Kiel, Germany
[3] Departamento de Astrofísica Molecular e Infrarroja, Instituto de Estructura de la Materia, CSIC, Calle Serrano 121, 28006 Madrid, Spain

Received 18 December 2006 / Accepted 23 January 2007

ABSTRACT

Context. Astronomical spectra of hot molecular clouds in the wavelength range from centimeter to submillimeter show a huge number of rotational lines due to the emission of complex organic molecules, and a large fraction of these lines are unidentified. The assignment of these unidentified lines to new molecules, to known molecules in excited states, or to their isotopologues requires a good knowledge of the spectroscopic parameters of these molecules.
Aims. We present the experimental study of the spectroscopic properties of ^{13}C-substituted ethyl cyanide $^{13}CH_3CH_2CN$, $CH_3{}^{13}CH_2CN$, and $CH_3CH_2{}^{13}CN$.
Methods. The rotational spectra of the three species in the ground state have been measured in the frequency ranges from 5 to 26 GHz using waveguide Fourier transform spectrometers and from 160 to 360 GHz using a source-modulated spectrometer employing backward-wave oscillators (BWOs).
Results. A new accurate set of spectroscopic constants has been determined for each isotopic species. This permits prediction of the position of rotational lines that are best suited for detection with an accuracy of a few hundreds of kHz. The three isotopologues have been detected in an Orion IRc2 IRAM survey via several hundred of lines, illustrating that many "unidentified" bands are definitely due to isotopologues of known molecules.

Key words. line: identification – methods: laboratory – molecular data – ISM: molecules – radio lines: ISM – submillimeter

1. Introduction

Radio spectra of hot molecular clouds (HMCs) exhibit thousands of rotational lines due to the emission of the molecules present in the clouds. Numerous spectral surveys of the chemically richest HMCs (e.g. in Orion, Sagittarius, etc.) have been performed in all the atmospheric spectral windows from 8 to 950 GHz (e.g. Nummelin et al. 1998; Schilke et al. 2001; White et al. 2003; Comito et al. 2005). These surveys show that the spectra are very dense. A large number of molecules have been identified in HMCs and are responsible for the observed emission lines. A non-exhaustive list of complex molecules detected in HMCs includes methyl formate (CH_3OCHO), acetic acid (CH_3COOH), glycoladehyde (CH_2OHCHO), dimethylether (CH_3OCH_3), methyl cyanide (CH_3CN), and ethyl cyanide (CH_3CH_2CN).

Most of these molecules have also been detected in warm gas around the low-mass protostar IRAS16293-2442 (Cazaux et al. 2003). Some molecules with a large spatial scale have been detected recently in emission and/or absorption: propenal (CH_2CHCHO) and propanal (CH_3CH_2CHO) (Hollis et al. 2004a), acetamide (CH_3CONH_2) (Hollis et al. 2006), and glycoladehyde (Hollis et al. 2004b). Because of the high temperature in HMCs, the low-lying vibrational or torsional state of large molecules can be significantly populated. Transitions from these vibrationally excited states have been detected in Sgr B2(N-LMH) for C_2H_3CN, CH_3CH_2OH (Nummelin et al. 1998), or CH_3CH_2CN (Merhinger et al. 2004). Finally, isotopic species of the most abundant molecules such as CO, SO, SO_2, CH_3OH, H_2CO, NH_3, HNCO, CH_3CN, HC_3N, are commonly observed in various astrophysical environments (e.g., Comito et al. 2005; Friedel et al. 2004 for HMCs).

However, a large number of lines in the interstellar spectra remain unidentified. In the Lovas catalogue (Lovas 2004), the unidentified lines (hereafter "U" lines) represent 16% of the observed lines. In most recent surveys of Orion KL and Sgr B2(N), the percentage of unidentified lines is about 8 to 20% (e.g. Nummelin et al. 1998; Schilke et al. 2001; Comito et al. 2005). However, the 3 mm survey of Sgr B2(N) performed by Friedel et al. (2004) with the BIMA array, in which 55% of the observed lines are unidentified, shows that the number of

⋆ Full Tables 6–8 are only available in electronic form at the CDS via anonymous ftp to cdsarc.u-strasbg.fr (130.79.125.5) or via http://cdsweb.u-strasbg.fr/cgi-bin/qcat?J/A+A/466/255
⋆⋆ Tables 3–5, 9–11 and a sample page of Tables 6–8 are only available in electronic form at http://www.aanda.org

"U" lines tends to increase with higher sensitivity and smaller beam size, since spectral confusion is avoided and more (weak) lines are consequentely observed. These "U" lines can be due (i) to new molecules, (ii) to vibrationally excited transitions from abundant molecules present in the ground state, (iii) to isotopologues of abundant molecules. However, at the moment, the lack of experimental data on excited states and isotopologues of large molecules prevents their identification in interstellar spectra. Since they contribute to the spectral congestion of the mm and submm spectra, it thus appears important to be able to identify these "U" lines confidently. This will "clean" the spectra and thus ease the search for new molecules. It will also give interesting information on the physical conditions and on the chemical processing going on in the HMCs. If the lines are due to excited state emission from known molecules, it allows us to trace the deepest regions of the clouds. The study of isotopologues gives information on the isotopic ratios and precise determination of abundances.

We present here an experimental study of the ground-state rotational spectrum of ^{13}C-substituted ethyl cyanide (CH_3CH_2CN). Ethyl cyanide is an abundant molecule observed in several hot molecular clouds via several hundreds of lines in the frequency range from 40 to 950 GHz. In hot molecular clouds, its column density is of the order of 10^{15}–10^{17} cm^{-2} (Mehringer & Snyder 1996; Miao & Snyder 1997). Mehringer et al. (2004) have detected transition from the first bending and torsional excited state of ethyl cyanide in Sgr B2(N-LMH). It has also been detected in the low-mass star-forming region IRAS 16293 with an abundance of about 9×10^{14} cm^{-2} (Cazaux et al. 2003). The ^{13}C-substituted ethyl cyanide dipole moment, which can be approximated to the value of the ^{12}C species, μ_a = 3.85 Debye and μ_b = 1.23 Debye (Heise et al. 1973), is large. Consequently, lines from isotopologues of ethyl cyanide are intense and should be observable towards sources having a large amount of ethyl cyanide, such as Orion or Sgr B2. ^{13}C-substituted ethyl cyanide has been studied by Heise et al. (1973). They measured a few small-J transitions in the microwave range (8–40 GHz) of $^{13}CH_3CH_2CN$, $CH_3{}^{13}CH_2CN$, and $CH_3CH_2{}^{13}CN$ and deduced the rotational constants and the quadrupole coupling constant for each species. In order to be able to calculate reliable prediction of the line positions at high frequency, we performed new measurements of these species in the 8–26 GHz and in the 160–360 GHz frequency range. The experimental setup is presented in Sect. 2, the data analysis and the results, in Sect. 3, and both are discussed in Sect. 4. The detection of the three isotopologues in Orion IRc2 is presented in Sects. 5 and 6.

2. Experiments

The samples of the isotopic ethyl cyanides $^{13}CH_3CH_2CN$ and $CH_3^{13}CH_2CN$ were prepared from the corresponding ^{13}C-substituted ethyl iodides, $^{13}CH_3CH_2I$ and $CH_3^{13}CH_2I$ (both 90% C-13, Sharp & Dohme, München), respectively, by a modified Kolbe-reaction (Autorenkollektiv, Organikum (8. Auflage), S.202, VEW Deutscher Verlag der Wissenschaften, Berlin 1968). For the species, $CH_3CH_2^{13}CN$, normal ethyl iodide from Merck (Darmstadt) and $Na^{13}CN$ was used. For all three syntheses, sodium cyanide was dispersed in a solution of the ethyl iodide in triethyleneglycol at room temperature. The mixture was then heated slowly to 110 °C and held at this temperature for 1 h. A magnetic stirrer was used to keep sodium cyanide well-dispersed throughout the mixture. The final product was isolated by distillation in vacuum and dried over P_2O_5. The purity of the sample was controlled gas chromatographically and the impurities found were isonitrile and ethyliodide. The sample purity of the ethylcanide was ca. 99.5%, so that additional purification was unnecessary.

In Kiel, the measurements in the centimeter-wave range were performed by means of microwave Fourier transform spectroscopy. Spectrometers in the ranges 8–18 GHz and 18–26.5 GHz were used, employing sample cells with a rectangular waveguide of length 12 m (Krüger et al. 1993; Sarka et al. 1997) and a circular waveguide cell of length 36 m (Meyer et al. 1991), respectively. The experiments were carried out at an ambient temperature and at gas pressures of ca. 0.1–0.2 Pa. Experimental transition frequencies were obtained from an analysis of the frequency-domain signals as obtained after Fourier transformation of the transient emission signal, using a peak-finder routine that yields line-center frequencies with an accuracy typically better than 20 kHz, depending on the strength of the line. In case of observed line splittings due to methyl internal rotation (AE-splittings), as well as the ^{14}N-nuclear quadrupole coupling, the experimental peak frequencies were corrected to obtain hypothetical unsplit line frequencies (without nuclear quadrupole hyperfine structure) for the A-species of internal rotation.

The millimeter spectra were recorded in the spectral range 160–360 GHz using a source-modulated spectrometer employing phase-stabilized backwardwave oscillators (Russian Istok backwardwave oscillators). The signal was detected on an InSb He-cooled bolometer (see e.g. Willaert et al. 2006, for more details on the experimental setup). The accuracy of the measurements is better than 100 kHz. The measurements were performed at room temperature. The pressure in the absorption cell (stainless steel, 6 cm in diameter, 110 cm long) was about 20 mTorr (2.6 Pa) and typical line width was 700 kHz (*FWHM*).

3. Analysis

For each species, the rotational spectrum was fitted to a Watson's Hamiltonian using A and S-reduction in I^r representation (Watson 1977) and the spectroscopic parameters in both A and S reduction were determined (see Tables 1 and 2). The initial prediction of the millimeter spectrum was calculated from the rotational parameters (in A reduction) determined from previous spectroscopic measurements by Heise et al. (1973), and the quartic constants of the parent species were used. The prediction was then improved step by step as new identified lines were added to the fit. The same procedure was also used for the analysis of the microwave measurements, which was done separately first. Then the two sets of lines were fitted together using the calculated unsplit frequencies for lines with observed hyperfine structure and/or internal rotational splitting.

As in the case of ^{12}C-ethyl cyanide, ^{13}C-isotopologues of ethyl cyanide show a very dense and intense spectrum. Furthermore, the spectra are probably contaminated by lines from the main species and/or by lines from the low-frequency vibrationally excited states. Consequently, the measured spectra show a lot of lines, a large number of which appear to be blended or distorted. Such lines were not included in the fit. The experimental uncertainty of the measured lines was fixed to 20 kHz for the microwave data (below 40 GHz) and to 50 kHz for the millimeter data, except for few lines were it was fixed to 100 kHz (lines labelled with a star in the tables).

The spectroscopic parameters derived for each species and their uncertainty are presented in Tables 1 and 2 in S and

Table 1. Spectroscopic constants of the ground vibrational state of ^{13}C-CH_3CH_2CN, S-reduction.

	$^{13}CH_3CH_2CN^{(a)}$		$CH_3^{13}CH_2CN^{(b)}$		$CH_3CH_2^{13}CN^{(c)}$	
	Value	Uncertainty	Value	Uncertainty	Value	Uncertainty
A/MHz	27 342.6493	(18)	27 045.8625	(16)	27 635.4314	(17)
B/MHz	4598.04 294	(37)	4697.93 650	(36)	4689.88 817	(27)
C/MHz	4133.76 933	(33)	4207.12 530	(33)	4214.80 409	(25)
D_J/kHz	2.93 368	(28)	2.92 691	(40)	2.96 968	(22)
D_{JK}/kHz	–48.0110	(23)	–44.6051	(16)	–47.4475	(19)
D_K/kHz	546.013	(12)	525.451	(15)	553.632	(40)
d_1/Hz	–662.479	(54)	–684.022	(85)	–676.592	(35)
d_2/Hz	–30.335	(35)	–34.513	(36)	–31.932	(14)
H_J/Hz	0.00 9254	(76)	0.01 044	(15)	0.00 8702	(57)
H_{JK}/Hz	–0.12 574	(111)	–0.0370	(11)	–0.12 048	(59)
H_{KJ}/Hz	–1.5554	(25)	–1.5755	(36)	–1.5001	(16)
H_K/Hz	30.344	(40)	27.710	(59)	30.26	(27)
h_1/mHz	3.623	(20)	3.883	(48)	3.684	(15)
h_2/mHz	0.386	(19)	0.643	(26)	0.4937	(97)
h_3/mHz	0.0236	(49)	0.0483	(fixed)	0.0484	(27)

Standard deviation of the fits: $^{(a)}$ 24 kHz, $^{(b)}$ 32 kHz, $^{(c)}$ 23 kHz, see text for more details. Uncertainties given in parenthesis are in units of the last digit given, one standard deviation.

Table 2. Spectroscopic constants of the ground vibrational state of ^{13}C-CH_3CH_2CN, A-reduction.

	$^{13}CH_3CH_2CN^{(a)}$		$CH_3^{13}CH_2CN^{(b)}$		$CH_3CH_2^{13}CN^{(c)}$	
	Value	Uncertainty	Value	Uncertainty	Value	Uncertainty
A/MHz	27 342.6503	(20)	27 045.8630	(18)	27 635.4303	(19)
B/MHz	4598.06 735	(39)	4697.96 236	(40)	4689.91 341	(31)
C/MHz	4133.74 505	(37)	4207.10 003	(35)	4214.77 921	(29)
Δ_J/kHz	2.99 463	(31)	2.99 599	(45)	3.03 369	(25)
Δ_{JK}/kHz	–48.3778	(23)	–45.0189	(17)	–47.8322	(20)
Δ_K/kHz	546.335	(13)	525.801	(17)	553.930	(45)
δ_J/kHz	0.66 2503	(56)	0.68 4149	(84)	0.67 6665	(36)
δ_K/kHz	12.097	(14)	12.749	(14)	12.5104	(59)
Φ_J/Hz	0.010157	(90)	0.01169	(18)	0.009812	(68)
Φ_{JK}/Hz	–0.06061	(89)	0.03828	(13)	–0.0852	(35)
Φ_{KJ}/Hz	–1.7894	(28)	–1.827	(39)	–1.637	(12)
Φ_K/Hz	30.558	(44)	27.880	(64)	29.95	(30)
ϕ_J/Hz	0.003662	(18)	0.003886	(52)	0.003647	(17)
ϕ_{JK}/Hz	0.0798	(83)	0.143	(10)	0.1329	(36)
ϕ_K/Hz	4.7551	(fixed)	4.7551	(fixed)	2.77	(23)

Standard deviation of the fits: $^{(a)}$ 27 kHz, $^{(b)}$ 37 kHz, $^{(c)}$ 23 kHz, see text for more details. Uncertainties given in parenthesis are in units of the last digit given, one standard deviation.

A-reduction, respectively. They are slightly better-determined in S-reduction than in A-reduction (see below for a detailed discussion for each species). To check this, we used GAUSSIAN 03 (Frisch et al. 2003) to calculate the reduction parameters s_{111} (Watson 1977) using ab initio (B3LYP/cc-pVTZ) harmonic force field. This parameter is indeed slightly smaller in the S-reduction ($s_{111}(S) = 0.11 \times 10^{-6}$) than in the A-reduction ($s_{111}(A) = 0.34\times10^{-6}$). Consequently, we present the list of the measured transitions and the results of the fit using S-reduction for the three species. The tables are available as online material (Tables 3−5). In both A and S-reduction, the standard deviation of the fits is within the experimental uncertainty (see below).

For $^{13}CH_3CH_2CN$, 193 lines were included in the fit (Table 3), including μ_a and μ_b transitions (136 and 57, respectively). Twenty-three lines are fitted below 40 GHz with $0 \leq J \leq 33$ and with a K_a value up to 8. In the 160−360 GHz frequency range, 170 lines are assigned with $10 \leq J \leq 51$ and with a K_a value up to 24. The standard deviation of the fit in S-reduction is 24 kHz. All the S-parameters are well-determined. In A-reduction, using the same list of measured lines, all the parameters are also well-determined except for h_K, which we fixed to the value of the ^{12}C-species given by Pearson et al. (1994). The standard deviation of the fit in A-reduction is 27 kHz.

A total of 161 transitions were assigned and included in the fit for $CH_3^{13}CH_2CN$, 84 μ_a transitions, and 77 μ_b transitions (Table 4). The fit includes 62 lines in the low-frequency range (below 40 GHz) with $0 \leq J \leq 41$ and a K_a value up to 8 and 99 lines in the 173−360 GHz frequency range with $8 \leq J \leq 69$ and a K_a value up to 32. In S-reduction all the parameters are well-determined except for h_3. Its value has been fixed to the value of the main isotopic species that was calculated from the parameters in the A-reduction given by Pearson et al. (1994). The resulting fit has a standard deviation of 32 kHz. In A-reduction, all parameters except for h_K are well-determined. As for $^{13}CH_3CH_2CN$, the h_K value was fixed to the value of the ^{12}C-species given by Pearson et al. (1994). The standard deviation of the fit in A-reduction is 37 kHz.

For $CH_3CH_2^{13}CN$, the fit includes 208 lines, 81 μ_a transitions, and 127 μ_b transitions (Table 5). Below 40 GHz, 113 transitions

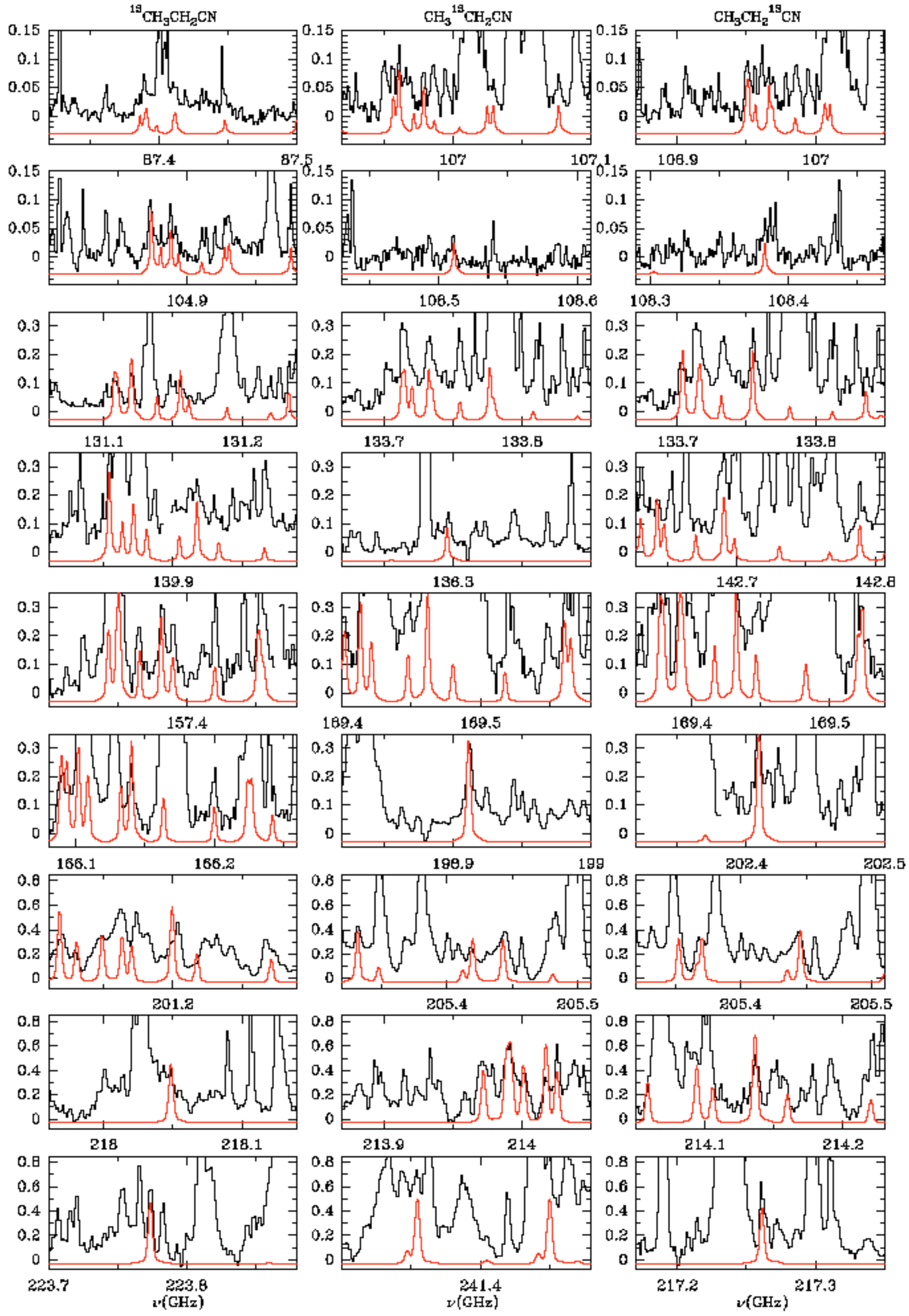

Fig. 1. ^{13}C-ethyl cyanide isotopologues detection in Orion. The spectra in all figures are in units of antenna temperature, T_A^*, corrected for atmospheric absorption and spillover losses.

are assigned with $0 \leq J \leq 60$ and a K_a value up to 10. In the 255−360 GHz frequency range, 95 transitions are assigned with $6 \leq J \leq 50$ and a K_a value up to 27. All the parameters are well-determined both in S and A-reduction. The standard deviation is 23kHz for both fits in A and S-reduction.

4. Discussion

The most intense rotational transitions of ethyl cyanide occur around 238, 333, and 407 GHz for temperatures of 100, 200 and 300 K, respectively, corresponding to J values of 25, 36, and 45, respectively. The rotational temperature of ethyl cyanide derived from the observations of hot cores is usually in the range 150−250 K with 200 K as the most frequent value. However, in low-mass star-forming regions such as IRAS 16293, the temperature is much lower with T_{rot} = 54 K (Cazaux et al. 2003).

Our measurements cover the spectral region at which the maximum of emission occurs at interstellar temperatures and also span the range of J value expected to be the most intense. Using the A-reduction, we have predicted the frequency of rotational transitions for each isotopologues up to 600 GHz and for $J \leq 60$. A short sample of the prediction is shown in the online section for each of three isotopologues (Tables 6−8), the entire tables are available in electronic form at the CDS. The error on the frequency given in the tables is the standard deviation. To get an estimate of the "true" error it must be multiplied by a factor 3, for the strongest lines to 10, for the weakest lines. Because the spectroscopic parameters are determined better for $CH_3CH_2^{13}CN$ than for the other species, the prediction of its rotational lines is better. However, the general trend is that for the lines that are the most suitable for detection, i.e. the strongest lines having J value up to ~50 and a low K_a value, the error on the predicted frequencies is a few hundred kHz, suitable for line identification in the insterstellar spectra. The error is larger for the weakest lines and increases as J and K_a become larger, i.e., as the frequency increases. Using the SPCAT program from Pickett (1998), we calculated the lines frequency in S-reduction for the three species. The frequencies predicted using A or S-reduction agree within 100 kHz for most of the lines. Only the weakest transitions and transitions with a high J value show higher discrepancy. However, the frequency difference is smaller than 500 kHz for transitions with $J \gtrsim 40$ and as high as 1 MHz for $J \gtrsim 55$.

5. Astronomical observations

The observations were carried out using the IRAM 30 m radio telescope during 2004 September (3 mm and 1.3 mm), 2005 March (2 mm), and 2005 April (3 mm and 1.3 mm). Four SiS receivers operating at 3, 2, and 1.3 mm were used simultaneously. Each receiver was tuned to a single sideband with image rejections within 20−27 dB (3 mm recievers), 12−16 dB (2 mm recievers), and 13 dB (1.3 mm recievers).

System temperatures were 100−350 K for the 3 mm recievers, 200−500 K for the 2 mm recievers and 200−800 K for the 1.3 mm recievers, depending on the observed frequency, the weather, and the source elevation. The intensity scale was calibrated using two absorbers at different temperatures and using the Atmosphere Transmission Model ATM (Cernicharo 1985; Pardo et al. 2001).

Pointing and focus were regularly checked on the nearby quasar 0420-014. The observations were made in the balanced wobbler-switching mode, with a wobbling period of 0.5 Hz and a beam throw of ±240″. The backends were two filter banks with 512 MHz bandwidth and 1 MHz resolution and a correlator divided into two bands of 512 MHz bandwidth and 1.25 MHz resolution. We pointed toward the position $\alpha = 5^h35^m14.4^s$, $\delta = -5°22'30.0s''$ (2000) corresponding to Orion IRc2. The detailed procedure used for the analysis of the line survey is described in Tercero et al. (in preparation). Figure 1 shows selected lines of the three ^{13}C isotopologues of CH_3CH_2CN. Observed parameters for all observed lines of these three isotopologues in the line survey of Tercero et al. (in preparation) are given in Tables 9−11.

6. Astronomical modelling

In agreement with previous observations of Orion, four well defined kinematic regions are implied by the observed velocities and line widths: (i) the narrow ambient cloud feature at $v_{LSR} \simeq 9$ km s^{-1} and characterized by line widths of $\lesssim 5$ km s^{-1} forming a N-S *extended ridge*; (ii) a quiescent, compact region, *compact ridge*, ($v_{LSR} \simeq 8$ km s^{-1}, $\Delta v \simeq 3$ km s^{-1}) identified for the first time by Johansson et al. (1984); (iii) the more turbulent and compact *plateau* ($v_{LSR} \simeq 6$−10 km s^{-1}, $\Delta v \gtrsim 25$ km s^{-1}); (iv) the *hot core* component ($v_{LSR} \simeq 3$−5 km s^{-1}, $\Delta v \lesssim 10$−15 km s^{-1}) first observed in ammonia emission (Morris et al. 1980). These components correspond to regions with differing physical and chemical conditions (Blake et al. 1987, 1996).

In modelling the emission from the isotopologues of CH_3CH_2CN, we find that a two-component model is enough to reproduce all line intensities and profiles reasonably well: the hot core component and the plateau. For the core a column density of 1.6×10^{15} cm^{-2}, a linewidth of 5 km s^{-1} and a rotational temperature of 300 K are the best parameters for reproducing the bulk of the ethyl cyanide emission. A broad velocity component is needed to fully reproduce the observations. It corresponds to the plateau for which we obtain a column density of 6×10^{13} cm^{-2}, a rotational temperature of 150 K, and a linewidth of 20 km s^{-1}. For the core component we assumed a source with uniform brightness temperature and a diameter of 7″ placed 3″ from the pointed position (the observations were pointed towards IRc2, while the CN bearing species seems to come from a small region 3″ North.) For the plateau component we assumed a size for the source of 30″. A first look at the main isotope's observed lines indicate that the column density to explain them will imply that some lines will not be optically thin and the derived isotopic ^{12}C/^{13}C abundance ratio could be >30. The detailed modelling of ethyl cyanide including the main isotope, the vibrationally exicted states, and all spectroscopically known isotopologues, will be published elsewhere (Tercero et al. in preparation).

Figure 1 shows selected observed lines of the three ^{13}C isotopologues, together with the model results. It can be seen that the agreement between observations and the model is very good. Tables 9−11 gives the model predictions, observed intensities and frequencies, and predicted frequencies from the rotational constants obtained in this paper, for all lines of the three isotopes that are not strongly blended with other lines. It is worth noting that the three isotopologues of ethyl cyanide contribute with more than 700 lines in the 80−280 GHz domain covered by the Orion line survey of Tercero et al. (in preparation).

Acknowledgements. This work was supported by the Programe National "PhysicoChimie du Milieu Interstellaire" and by the European Research Training Network "Molecular Universe" (MRTN-CT-2004-512302).

References

Blake, G. A., Sutton, E. C., Masson, C. R., & Philips, T. H. 1987, ApJ, 315, 621
Blake, G. A., Mundy, L. G., Carlstrom, J. E., et al. 1996, ApJ, 472, L49
Cazaux, S., Tielens, A. G. G. M., Ceccarelli, C., et al. 2003, A&A, 593, L51
Cernicharo, J. 1985, Internal IRAM report (Granada: IRAM)
Comito, C., Schilke, P., Phillips, T. G., et al. 2005, ApJS, 156, 127
Friedel, D. N., Snyder, L. E., Turner, B. E., et al. 2004, ApJ, 600, 234
Frisch, M. J., Trucks, G. W., Schlegel, H. B., et al. 2003, GAUSSIAN 03, Revision B.04, Gaussian, Inc., Pittsburgh PA
Fukuyama, Y., Odashima, H., Takagi, K., et al. 1996, ApJSS, 104, 329
Heise, H. M., Lutz, H., & Dreizler, H. 1973, Z. Naturforsch., 29a, 1345
Hollis, J. M., Jewell, P. R., Lovas, F. J., et al. 2004a, ApJ, 610, L21
Hollis, J. M., Jewell, P. R., Lovas, F. J., et al. 2004b, ApJ, 613, L45
Hollis, J. M., Lovas, F. J., Remijan, A. J., et al. 2006, ApJ, 643, L25
Johansson, L. E. B., Andersson, C., Elldér, J., et al. 1984, A&A, 130, 227
Krüger, M., Harder, H., Gerke, C., et al. 1993, Z. Naturforsch. A, 43, 737
Lovas, F. J. 2004, J. Phys. Chem. Ref. Data, 33, 177
Miao, Y., & Snyder, L. E. 1997, ApJ, 480, L67
Mehringer, D. M., & Snyder, L. E. 1996, ApJ, 471, 897
Mehringer, D. M., Pearson, J. C., Keene, J., et al. 2004, ApJ, 608, 306
Meyer, V., Jäger, W., Schwarz, R., et al. 1991, Z. Naturforsch. A, 46, 445
Morris, M., Palmer, P., & Zuckerman, B. 1980, ApJ, 237, 1
Nummelin, A., Bergman, P., Hjalmarson, A., et al. 1998, ApJSS, 117, 427
Pardo, J. R., Cernicharo, J., & Serabyn, E. 2001, E. IEEE Tras. Antennas and Propagation, 49, 12
Pearson, J. C., Sastry, K. V. L. N., Herbst, E., & De Lucia, F. C. 1994, ApJSS, 93, 589
Pickett, H. M., Poynter, R. L., Cohen, E. A., et al. 1998, J. Quant. Spectrosc., Radiat. Trans., 60, 883
Remijan, A., Sutton, E. C., Snyder, L. E., et al. 2004, ApJ, 606, 917
Sarka, K., Papoušek, D., Demaison, J., et al. 1997, in Advanced Series in Physical Chemistry, Vol. 9, ed. D. Papoušek (Singapore: World Scientific Publishing)
Schilke, P., Benford, D. J., Hunter, T. R., et al. 2001, ApJSS, 132, 281
Watson, J. K. G. 1977, in Vibrational Spectra and Molecular Structure, 6, 1, Elsevier, Amsterdam
White, G. J., Araki, M., Greaves, J. S., Ohishi, M., & Higginbottom, N. S. 2003, A&A, 407, 589
Willaert, F., Møllendal, H., Alekseev, E., et al. 2006, J. Mol. Spec., 795, 4

Online Material

Table 3. Measured transitions of the ground vibrational state of $^{13}CH_3CH_2CN$.

Transition						Obs. Freq.	obs.- calc	S	Dipole	E_u
J'	K'_a	K'_c	J''	K''_a	K''_c	(MHz)	(MHz)			(cm^{-1})
1	0	1	0	0	0	8731.787	–0.014	1.0000	a	0.291
13	2	11	13	2	12	8820.637	–0.001	0.5509	a	29.814
6	1	5	6	1	6	9741.825	0.002	0.3102	a	7.042
22	3	19	22	3	20	10142.777	–0.036	0.7152	a	81.064
14	2	12	14	2	13	11484.067	0.010	0.5035	a	33.963
23	3	20	23	3	21	12811.652	0.004	0.6706	a	87.863
30	5	26	29	6	23	12888.797	–0.035	4.7812	b	154.899
7	1	6	7	1	7	12981.545	–0.010	2.6900	a	9.131
4	0	4	3	1	3	13241.366	–0.045	1.6139	b	2.909
30	5	25	29	6	24	13523.629	0.015	4.7844	b	154.919
15	2	13	15	2	14	14614.108	0.018	0.4619	a	38.414
33	4	29	33	4	30	15275.167	0.002	0.8033	a	176.688
8	1	7	8	1	8	16676.336	0.006	0.2378	a	11.518
2	1	2	1	1	1	16999.464	–0.007	1.5000	a	1.617
2	0	2	1	0	1	17456.478	–0.017	1.9998	a	0.874
2	1	1	1	1	0	17927.960	–0.015	1.5000	a	1.663
1	1	0	1	0	1	23208.440	0.013	1.5000	b	1.065
2	1	1	2	0	2	23679.910	0.003	2.4746	b	1.663
3	0	3	2	0	2	26167.010	0.018	2.9994	a	1.746
3	2	2	2	2	1	26196.320	0.045	1.6667	a	4.813
3	2	1	2	2	0	26224.320*	–0.077	1.6667	a	4.814
1	1	1	0	0	0	31475.950	–0.010	1.0000	b	1.050
2	1	2	1	0	1	39743.600	–0.029	1.5000	b	1.617
19	1	19	18	1	18	160026.237	0.003	18.9300	a	54.353
19	0	19	18	0	18	160670.979	–0.076	18.9406	a	54.251
19	1	19	18	0	18	163749.602	0.001	14.9503	b	54.353
19	2	18	18	2	17	164569.131	0.031	18.7719	a	58.174
19	8	12	18	8	11	166089.133	0.031	15.6320	a	104.369
19	9	11	18	9	10	166093.022	0.011	14.7372	a	117.359
19	7	13	18	7	12	166101.509	–0.012	16.4214	a	92.902
19	10	9	18	10	8	166108.275	–0.031	13.7372	a	131.866
19	11	9	18	11	8	166132.304	0.077	12.6319	a	147.887
19	6	14	18	6	13	166139.856	–0.021	17.1056	a	82.962
19	12	7	18	12	6	166163.093	–0.034	11.4213	a	165.416
19	13	6	18	13	5	166199.966	–0.001	10.1055	a	184.449
19	5	15	18	5	14	166223.974	0.022	17.6844	a	74.555
19	5	14	18	5	13	166226.873	–0.025	17.6844	a	74.55
19	14	6	18	14	5	166242.075	0.009	8.6844	a	204.980
19	15	4	18	15	3	166288.950	–0.004	7.1581	a	227.003
19	3	17	18	3	16	166292.896	0.021	18.5229	a	62.338
19	16	3	18	16	2	166340.300	0.001	5.5265	a	250.513
19	17	2	18	17	1	166395.875	0.018	3.7896	a	275.503
19	18	2	18	18	1	166455.400	–0.042	1.9474	a	301.966
19	4	15	18	4	14	166456.762	–0.036	18.1576	a	67.699
19	3	16	18	3	15	167484.066	–0.007	18.5249	a	62.490
19	1	18	18	1	17	167617.028	–0.016	18.8983	a	57.137
19	2	17	18	2	16	169635.261	–0.010	18.7983	a	59.240
51	6	45	51	5	46	200312.750	0.018	33.3052	b	415.494
25	1	24	24	2	23	200333.644	0.005	12.6546	b	96.551
24	0	24	23	1	23	200393.875	0.007	20.0546	b	85.159
10	3	8	9	2	7	200679.951	0.022	3.6961	b	22.931
31	11	21	32	10	22	200714.382	–0.015	3.6058	b	237.128
38	3	36	38	2	37	200763.718	–0.012	14.0305	b	222.469
27	5	22	27	4	23	200800.625	–0.013	14.7565	b	129.471
26	5	21	26	4	22	201821.081	0.030	14.0988	b	121.578
47	3	44	47	2	45	202443.284	0.054	21.9164	b	340.449
36	12	25	37	11	26	202489.130	0.029	4.3788	b	304.243
29	2	27	28	3	26	202590.950	0.012	8.6623	b	132.075
41	13	29	42	12	30	204255.377	–0.021	5.1537	b	380.156
46	14	32	47	13	35	206025.390	0.023	5.9295	b	464.859
25	10	16	26	9	17	207666.029	–0.071	2.6210	b	171.235
51	15	36	52	14	39	207810.182	0.048	6.7058	b	558.346
35	12	23	36	11	26	211217.493	–0.008	4.1583	b	293.745
40	13	27	41	12	30	212966.680	–0.029	4.9322	b	368.202
45	14	31	46	13	34	214714.901	0.030	5.7075	b	451.450
50	15	35	51	14	38	216473.279	–0.005	6.4834	b	543.483

Table 3. continued.

Transition						Obs. Freq.	obs.- calc	S	Dipole	E_u
J'	K'_a	K'_c	J''	K''_a	K''_c	(MHz)	(MHz)			(cm^{-1})
47	6	41	47	5	42	217173.407	–0.017	28.7146	b	357.302
29	11	18	30	10	21	218192.084	–0.001	3.1696	b	219.339
34	12	22	35	11	25	219942.900	0.044	3.9387	b	283.539
46	6	40	46	5	41	220951.757	0.012	27.7406	b	343.509
39	13	26	40	12	29	221675.619	0.008	4.7113	b	356.539
44	14	30	45	13	33	223402.661	–0.002	5.4858	b	438.332
45	6	39	45	5	40	224476.868	0.008	26.8213	b	330.016
49	15	34	50	14	37	225135.488	0.038	6.2613	b	528.911
54	16	38	55	15	41	226884.609	0.007	7.0372	b	628.266
28	11	17	29	10	20	226925.942	0.035	2.9537	b	210.882
50	3	47	50	2	48	228283.377	0.014	21.6854	b	383.454
33	12	21	34	11	24	228665.396	–0.064	3.7200	b	273.624
38	13	25	39	12	28	230382.355	0.005	4.4910	b	345.167
43	14	29	44	13	32	232088.953	0.007	5.2645	b	425.504
48	15	33	49	14	36	233796.798	–0.006	6.0394	b	514.628
28	1	28	27	1	27	234578.709	0.052	27.9332	a	114.840
28	0	28	27	0	27	234693.820	0.039	27.9342	a	114.825
53	16	37	54	15	40	235516.628	–0.073	6.8150	b	612.531
51	3	48	51	2	49	236657.801	–0.033	21.6461	b	398.325
28	2	27	27	2	26	240526.912	–0.011	27.8099	a	120.284
28	1	27	27	1	26	242178.053	0.020	27.8373	a	119.968
28	3	26	27	3	25	244390.469	0.044	27.6593	a	125.318
28	10	19	27	10	18	244788.651	0.029	24.4292	a	194.856
28	9	19	27	9	18	244799.020	0.072	25.1078	a	180.347
28	11	18	27	11	17	244799.620	–0.049	23.6792	a	210.882
28	12	16	27	12	15	244826.863	0.030	22.8577	a	228.420
28	8	21	27	8	20	244839.562	0.040	25.7149	a	167.363
28	13	16	27	13	15	244866.876	0.047	21.9649	a	247.465
28	14	15	27	14	14	244917.512	0.001	21.0005	a	268.010
28	7	21	27	7	20	244926.445	–0.062	26.2505	a	155.910
28	15	13	27	15	12	244977.411	–0.008	19.9648	a	290.050
28	16	12	27	16	11	245045.511	–0.021	18.8576	a	313.578
28	6	23	27	6	22	245089.645	0.043	26.7147	a	146.000
28	6	22	27	6	21	245094.088	0.040	26.7147	a	146.000
28	17	11	27	17	10	245121.106	–0.004	17.6790	a	338.588
28	18	11	27	18	10	245203.596	–0.009	16.4290	a	365.073
28	19	9	27	19	8	245292.588	–0.009	15.1075	a	393.026
28	5	24	27	5	23	245363.475	–0.051	27.1070	a	137.648
28	20	9	27	20	8	245387.747	–0.013	13.7146	a	422.440
28	5	23	27	5	22	245457.481	–0.067	27.1070	a	137.658
28	21	8	27	21	7	245488.826	–0.005	12.2503	a	453.306
28	4	25	27	4	24	245535.703	0.032	27.4254	a	130.841
28	22	7	27	22	6	245595.604	0.007	10.7145	a	485.618
28	23	6	27	23	5	245707.909	0.032	9.1074	a	519.365
28	24	4	27	24	3	245825.528	0.011	7.4288	a	554.541
28	4	24	27	4	23	246658.154	0.028	27.4273	a	131.000
28	2	26	27	2	25	248935.085	–0.012	27.8281	a	123.487
30	6	24	30	5	25	249174.110	–0.080	16.0047	b	163.231
31	6	26	31	5	27	249416.860	0.010	16.6299	b	172.285
28	3	25	27	3	24	249580.945	–0.017	27.6940	a	126.437
29	6	23	29	5	24	249657.780	0.002	15.3741	b	154.469
30	6	25	30	5	26	249761.030	–0.005	15.9963	b	163.230
30	3	28	29	3	27	261540.610	–0.025	29.6744	a	142.480
30	13	18	29	13	17	262339.703	–0.011	24.3673	a	264.675
30	6	24	29	6	23	262678.575	0.028	28.8004	a	163.231
30	5	26	29	5	25	262991.196	0.069	15.3004	a	154.899
30	4	27	29	4	26	263084.417	0.009	29.4619	a	148.100
30	5	25	29	5	24	263162.025*	–0.109	29.1664	a	146.14
31	2	30	30	2	29	265544.775	–0.021	30.8126	a	146.023
30	2	28	29	2	27	265968.621	–0.023	29.8165	a	140.947
31	1	30	30	1	29	266639.175*	0.119	30.8263	a	136.94
32	0	32	31	1	31	267416.117	–0.006	28.1913	b	139.97
32	1	32	31	1	31	267600.895	–0.014	31.9332	a	139.97
32	0	32	31	0	31	267648.854	–0.010	31.9335	a	139.96
32	1	32	31	0	31	267833.634	–0.016	28.1937	b	139.96
31	3	29	30	3	28	270083.054	0.007	30.6805	a	142.48

Table 3. continued.

J'	K'_a	K'_c	J''	K''_a	K''_c	Obs. Freq. (MHz)	obs.- calc (MHz)	S	Dipole	E_u (cm^{-1})
31	10	22	30	10	21	271014.330	0.003	27.7749	a	212.06
31	11	21	30	11	20	271015.430	0.008	27.0975	a	228.09
31	4	28	30	4	27	271843.387	–0.006	30.4780	a	148.10
31	5	26	30	5	25	272034.865	–0.018	30.1932	a	154.92
32	2	31	31	2	30	273858.241	0.012	31.8130	a	146.02
31	4	27	30	4	26	273902.663	–0.034	30.4840	a	148.36
31	2	29	30	2	28	274393.857	–0.002	30.8089	a	140.95
32	1	31	31	1	30	274796.266	–0.004	31.8238	a	145.83
33	0	33	32	1	32	275703.647	–0.018	29.2011	b	148.89
33	1	33	32	0	32	276034.933	–0.011	29.2029	b	148.89
32	3	30	31	3	29	278603.322	–0.029	31.6858	a	151.49
32	12	21	31	12	20	279772.356	0.006	27.5007	a	254.67
32	14	19	31	14	18	279859.510	–0.018	25.8757	a	294.27
32	16	16	31	16	15	279995.091	–0.020	24.0006	a	339.85
32	6	27	31	6	26	280262.780	0.001	30.8754	a	172.28
32	19	13	31	19	12	280267.080	–0.046	20.7193	a	419.32
32	6	26	31	6	25	280281.703	–0.002	30.8754	a	172.29
32	4	29	31	4	28	280589.844	–0.010	31.4929	a	157.17
32	5	28	31	5	27	280626.915	–0.006	31.2181	a	163.97
32	5	27	31	5	26	280923.629	–0.001	31.2183	a	163.99
33	2	32	32	2	31	282160.483	0.016	32.8132	a	155.16
32	2	30	31	2	29	282759.346	–0.006	31.8004	a	150.10
33	1	32	32	1	31	282958.925	0.008	32.8217	a	155.00
32	4	28	31	4	27	283048.455	–0.007	31.5014	a	157.50
34	1	34	33	1	33	284097.236	–0.014	33.9331	a	158.09
34	0	34	33	0	33	284127.747	–0.021	33.9333	a	158.09
33	9	25	32	9	24	288537.625	–0.043	30.5462	a	225.552
33	13	20	32	13	19	288542.025	0.023	27.8795	a	292.675
33	8	26	32	8	25	288624.850*	–0.076	31.0614	a	202.95
33	2	31	32	2	30	291067.998	–0.005	32.7913	a	169.241
34	3	32	33	3	31	295577.772	–0.010	33.6941	a	180.218
34	4	31	33	4	30	298038.650	–0.017	33.5192	a	186.119
34	5	30	33	5	29	298264.398	–0.001	33.2636	a	192.930
35	2	34	34	2	33	298735.381	0.031	34.8133	a	184.223
35	1	34	34	1	33	299303.327	0.005	34.8185	a	184.134
35	2	33	34	2	32	307534.084	0.001	34.7726	a	189.483
37	2	36	36	2	35	315276.922	0.004	36.8129	a	204.920
36	6	31	35	6	30	315491.883	0.054	35.0003	a	221.965
36	6	30	35	6	29	315558.436*	0.110	35.0004	a	211.45
37	1	36	36	1	35	315672.795	0.017	36.8162	a	204.920
36	5	32	35	5	31	315894.994	0.005	35.3038	a	213.710
38	1	38	37	1	37	317066.100	0.025	37.9329	a	208.226
38	0	38	37	0	37	317078.208	0.027	37.9330	a	208.225
38	1	38	37	0	37	317123.217	0.011	34.2383	a	208.226
15	5	10	14	4	11	337515.735*	0.087	6.0893	b	42.87
44	3	41	43	4	40	338832.968	–0.028	14.1851	b	299.871
38	8	31	38	7	32	341597.080	–0.071	19.8804	b	265.100
37	8	29	37	7	30	341845.924	0.010	19.2632	b	254.001
37	8	30	37	7	31	341861.311*	–0.104	19.2631	b	242.61
41	2	40	40	2	39	348284.689	0.025	40.8117	a	249.800
41	1	40	40	1	39	348468.256	0.021	40.8130	a	249.773
40	4	37	39	4	36	349933.000	–0.017	39.5739	a	251.839
42	1	42	41	1	41	350005.923	–0.013	41.9328	a	253.278
42	0	42	41	0	41	350010.627	–0.012	41.9328	a	253.278
40	6	35	39	6	34	350767.487	0.033	39.1002	a	267.001
40	6	34	39	6	33	350967.063	0.047	39.1004	a	267.027
40	5	36	39	5	35	351092.104	–0.002	39.3709	a	258.795
41	3	39	40	3	38	354343.168	0.004	40.7060	a	257.093
40	3	37	39	3	36	355723.668	0.024	39.7462	a	249.611
43	1	43	42	1	42	358236.456	–0.014	42.9327	a	265.228
43	0	43	42	0	42	358240.157	–0.016	42.9328	a	265.227

Table 4. Measured transitions of the ground vibrational state of $CH_3^{13}CH_2CN$.

Transition						Obs. Freq.	obs.- calc	S	Dipole	E_u
J'	K'_a	K'_c	J''	K''_a	K''_c	(MHz)	(MHz)			(cm^{-1})
1	0	1	0	0	0	8905.044	–0.006	1.0000	a	0.297
11	1	11	10	2	8	9481.367	–0.008	1.1558	b	19.775
39	5	34	39	5	35	9656.697	–0.019	1.0887	a	251.698
13	2	11	13	2	12	9913.694	0.007	0.5460	a	30.318
30	4	26	30	4	27	10040.036	–0.023	0.9171	a	150.964
6	1	5	6	1	6	10297.775	–0.022	0.3103	a	7.159
10	3	8	11	2	9	10934.004	0.013	1.6211	b	23.135
19	3	17	18	4	14	11641.784	–0.007	2.9697	b	63.330
8	1	7	7	2	6	12005.052	–0.036	1.5239	b	11.728
22	3	19	22	3	20	12116.649	0.002	0.7030	a	82.487
15	4	12	16	3	13	12748.766	0.021	2.3772	b	47.745
14	2	12	14	2	13	12872.438	0.002	0.4983	a	34.556
6	2	4	7	1	7	13027.601	0.011	0.8766	b	9.269
24	4	21	23	5	18	13135.700	0.027	3.7734	b	101.395
34	6	29	33	7	26	13375.237	–0.018	5.3335	b	204.243
12	1	12	11	2	9	13621.397	–0.006	1.1409	b	23.225
20	5	16	21	4	17	13663.533	–0.038	3.1486	b	81.296
7	1	6	7	1	7	13721.366	–0.014	0.2692	a	9.292
25	6	20	26	5	21	14111.813	0.024	3.9224	b	123.786
4	0	4	3	1	3	14383.683	0.011	3.1450	b	2.966
30	7	24	31	6	25	14408.589	0.017	4.6963	b	175.211
35	8	28	36	7	29	14685.542	–0.027	5.4698	b	235.563
35	8	27	36	7	30	14703.948	0.020	5.4697	b	235.563
41	5	36	41	5	37	14828.858	0.006	0.9956	a	276.067
24	4	20	23	5	19	15152.112	0.050	3.7862	b	101.460
15	2	14	14	3	11	15161.704	–0.014	2.2440	b	38.557
23	3	20	23	3	21	15240.446	–0.017	0.6576	a	89.433
32	4	28	32	4	29	15661.815	–0.008	0.8240	a	169.949
2	1	2	1	1	1	17319.429*	0.010	1.5000	a	1.620
2	0	2	1	0	1	17801.970*	–0.064	1.9998	a	0.891
2	1	1	1	1	0	18301.029	0.031	1.5000	a	1.669
24	3	21	24	3	22	18882.863	0.007	0.6153	a	96.692
4	2	3	5	1	4	19620.967	0.032	0.6473	b	5.985
14	1	14	13	2	11	19786.625	–0.014	1.0370	b	30.978
5	2	3	6	1	6	19871.579	0.018	0.7241	b	7.478
16	2	14	16	2	15	20308.852	–0.004	0.4200	a	43.957
20	3	18	19	4	15	20314.677	–0.015	3.1547	b	69.285
9	3	7	10	2	8	21018.173	0.006	1.3911	b	20.160
14	2	12	13	3	11	21138.489	–0.044	2.3321	b	34.556
15	1	15	14	2	12	21749.882	0.018	0.9612	b	35.281
19	1	19	18	2	16	21915.027	–0.007	0.6331	b	55.323
9	1	8	9	1	9	22000.678	–0.017	0.2140	a	14.466
25	4	22	24	5	19	22299.882	–0.002	3.9737	b	108.854
16	2	15	15	3	12	22363.699	–0.026	2.3607	b	43.280
14	4	11	15	3	12	22367.840	0.008	2.1573	b	43.280
30	5	26	29	6	23	22807.601	–0.005	4.7622	b	157.312
1	1	0	1	0	1	22838.291*	–0.007	1.5000	b	1.059
16	1	16	15	2	13	22943.481	–0.002	0.8781	b	39.867
9	1	8	8	2	7	22960.085	0.022	1.8613	b	14.466
18	1	18	17	2	15	23015.849	0.015	0.7106	b	49.888
25	3	22	25	3	23	23066.250	0.016	0.5760	a	104.263
2	1	1	2	0	2	23337.236	–0.026	2.4727	b	1.669
17	1	17	16	2	14	23363.507	–0.003	0.7932	b	44.737
14	4	10	15	3	13	23850.332	0.008	2.1485	b	43.281
3	1	2	3	0	3	24100.582	–0.018	3.4044	b	2.585
5	0	5	4	1	4	24125.648	0.005	2.2277	b	4.446
17	2	15	17	2	16	24800.110	0.002	0.3880	a	49.121
25	4	21	24	5	20	25052.940	0.039	3.9927	b	108.942
4	1	3	4	0	4	25145.986	0.005	4.2789	b	3.805
3	1	3	2	1	2	25974.033	–0.003	2.6666	a	2.487
1	1	1	0	0	0	31252.510*	–0.033	1.0000	b	1.042
2	1	2	1	0	1	39666.830*	–0.082	1.5000	b	1.620
20	1	20	19	0	19	173995.349	0.022	16.1379	b	61.039
20	2	19	19	2	18	176356.794	0.027	19.7769	a	65.074
21	0	21	20	1	20	178081.995	0.020	17.1280	b	66.979
20	9	12	19	9	11	178310.299	–0.005	15.9505	a	123.373

Table 4. continued.

Transition						Obs. Freq.	obs.- calc	S	Dipole	E_u
J'	K'_a	K'_c	J''	K''_a	K''_c	(MHz)	(MHz)			(cm^{-1})
20	8	13	19	8	12	178315.818	0.001	16.8005	a	110.600
20	10	11	19	10	10	178318.655	0.013	15.0004	a	137.638
20	11	10	19	11	9	178337.208	0.038	13.9504	a	153.393
20	7	14	19	7	13	178341.762	0.019	17.5505	a	99.326
20	12	8	19	12	7	178363.807*	0.100	12.8004	a	170.631
20	13	8	19	13	7	178396.995*	0.112	11.5503	a	189.349
20	6	15	19	6	14	178400.958*	0.118	18.2004	a	89.556
20	14	7	19	14	6	178435.877	0.081	10.2003	a	209.541
20	3	18	19	3	17	178510.736	0.040	19.5448	a	69.285
20	5	16	19	5	15	178518.421	0.009	18.7502	a	81.296
20	4	17	19	4	16	178701.651	0.042	19.1995	a	74.557
20	1	19	19	1	18	179348.625	0.016	19.8827	a	64.225
21	1	21	20	1	20	179811.950	–0.012	20.9295	a	67.037
21	0	21	20	0	20	180219.881	0.027	20.9348	a	66.979
20	3	17	19	3	16	180294.217	–0.026	19.5492	a	69.528
21	1	21	20	0	20	181949.853	0.012	17.1636	b	67.037
20	2	18	19	2	17	182346.464	–0.001	19.8086	a	66.451
34	3	32	34	2	33	182384.257	–0.029	13.3793	b	183.493
16	2	15	15	1	14	182426.658	0.020	6.2256	b	43.280
23	1	22	22	2	21	184902.128	0.025	11.0620	b	83.871
21	2	20	20	2	19	184998.569	–0.004	20.7831	a	71.245
21	9	13	22	8	14	186728.043	0.022	2.0760	b	129.618
21	9	13	20	9	12	187229.852	0.033	17.1433	a	129.618
21	10	11	20	10	10	187235.861	0.007	16.2386	a	143.884
21	8	14	20	8	13	187239.436	–0.003	17.9529	a	116.846
21	11	10	20	11	9	187253.313	0.006	15.2385	a	159.639
21	7	15	20	7	14	187272.318	–0.001	18.6671	a	105.573
21	12	9	20	12	8	187279.700	0.047	14.1433	a	176.878
21	13	9	20	13	8	187313.411*	0.102	12.9528	a	195.598
21	14	7	20	14	6	187353.281	0.048	11.6670	a	215.791
21	15	7	20	15	6	187398.821*	0.104	10.2860	a	237.453
21	3	19	20	3	18	187400.405*	0.080	20.5649	a	75.536
21	16	5	20	16	4	187449.377*	0.120	8.8098	a	260.578
21	5	17	20	5	16	187480.600	0.044	19.8097	a	87.550
21	5	16	20	5	15	187490.829	0.008	19.8097	a	87.551
21	4	18	20	4	17	187679.400	–0.012	20.2374	a	80.817
21	1	20	20	1	19	187870.493	0.024	20.8747	a	70.492
21	4	17	20	4	16	187900.112	–0.020	20.2375	a	80.841
21	3	18	20	3	17	189588.113	0.016	20.5716	a	75.852
21	2	19	20	2	18	191453.322	–0.007	20.8164	a	72.837
24	1	23	23	2	22	195818.289	0.093	12.0843	b	90.980
25	5	21	25	4	22	200978.255	–0.078	13.4867	b	115.558
21	5	16	21	4	17	201170.954	–0.069	11.0038	b	87.551
25	0	25	24	1	24	212814.767	–0.001	21.2390	b	93.817
25	1	25	24	1	24	213528.288	–0.015	24.9307	a	93.841
25	2	24	24	2	23	219359.808	0.006	24.7989	a	98.797
25	1	24	24	1	23	221481.444	0.016	24.8432	a	98.368
17	9	9	18	8	10	222436.415	0.018	1.2591	b	106.422
26	1	26	25	0	25	222657.909	–0.025	22.2678	b	101.244
27	11	17	28	10	18	222729.986	–0.036	2.7400	b	203.361
25	3	23	24	3	22	222791.608	–0.006	24.6257	a	103.494
47	15	33	48	14	34	222874.167	–0.024	5.8161	b	504.293
25	8	18	24	8	17	222945.684	–0.037	22.4406	a	144.806
25	6	20	24	6	19	223146.875	0.045	23.5604	a	123.786
25	5	21	24	5	20	223377.774	–0.034	24.0000	a	115.558
25	20	5	24	20	4	223408.176*	–0.101	9.0003	a	395.599
25	5	20	24	5	19	223426.457	–0.029	24.0000	a	115.563
25	21	4	24	21	3	223492.281	–0.031	7.3602	a	425.950
25	22	3	24	22	2	223581.060	0.022	5.6402	a	457.722
25	4	22	24	4	21	223594.357	–0.021	24.3580	a	108.854
13	3	11	12	2	10	223653.826	–0.054	4.2335	b	33.851
25	23	3	24	23	2	223674.332	0.028	3.8401	a	490.908
25	4	21	24	4	20	224297.077	–0.029	24.3588	a	108.942
30	2	28	29	3	27	226172.501	–0.049	9.9797	b	143.692
41	4	37	40	5	36	226833.862	0.052	7.5143	b	270.892
25	3	22	24	3	21	226974.967	–0.026	24.6495	a	104.263

Table 4. continued.

Transition						Obs. Freq.	obs.- calc	S	Dipole	E_u
J'	K'_a	K'_c	J''	K''_a	K''_c	(MHz)	(MHz)			(cm^{-1})
25	2	23	24	2	22	227385.495	–0.013	24.8276	a	101.387
8	4	5	7	3	4	229304.243	–0.035	4.0457	b	22.753
8	4	4	7	3	5	229321.787*	0.125	4.0455	b	22.753
11	8	4	12	7	5	231101.016	0.076	0.4208	b	67.780
16	9	8	17	8	9	231353.174	–0.046	1.0673	b	101.366
49	3	46	49	2	47	231542.472*	–0.154	20.8620	b	375.864
13	3	10	12	2	11	231728.449	0.046	4.0071	b	33.872
46	15	32	47	14	33	231731.580	0.025	5.5954	b	490.320
25	2	24	24	1	23	234341.014	0.033	13.4227	b	98.797
27	3	25	26	3	24	240366.920	–0.012	26.6467	a	119.237
27	7	21	26	7	20	240900.160	–0.019	25.1858	a	149.313
27	6	22	26	6	21	241070.960	–0.057	25.6671	a	139.570
27	6	21	26	6	20	241075.450*	–0.084	25.6671	a	139.570
27	5	23	26	5	22	241354.180	–0.053	26.0739	a	131.359
27	5	22	26	5	21	241449.960	–0.036	26.0740	a	131.370
27	4	23	26	4	22	242677.730	–0.063	26.4061	a	124.825
28	5	23	27	5	22	250479.760	–0.071	27.1070	a	139.725
17	3	15	16	2	14	250482.920	0.005	5.0273	b	52.312
30	1	30	29	0	29	255854.360*	–0.084	26.3207	b	133.662
18	3	16	17	2	15	256380.340	0.012	5.2588	b	57.673
15	10	5	16	9	8	284979.200	0.019	0.6624	b	110.872
25	3	23	24	2	22	290534.920	0.000	7.7052	b	103.494
68	7	62	68	6	63	298152.660*	0.064	39.7600	b	736.517
69	7	63	69	6	64	301242.380*	–0.054	40.1274	b	757.101
28	3	26	27	2	25	302996.360	–0.019	9.4131	b	127.546
29	3	27	28	2	26	307130.700	–0.040	10.0946	b	136.147
38	31	7	37	31	6	341021.260	–0.064	12.7109	a	930.840
39	16	23	38	16	22	347838.580*	0.059	32.4369	a	423.970
40	32	8	39	32	7	359108.350	0.046	14.4004	a	1000.083

Table 5. Measured transitions of the ground vibrational state of $CH_3CH_2^{13}CN$.

Transition						Obs. Freq.	obs.- calc	S	Dipole	E_u
J'	K'_a	K'_c	J''	K''_a	K''_c	(MHz)	(MHz)			(cm^{-1})
59	7	52	59	7	53	8039.170	–0.030	1.3896	a	565.494
49	6	43	49	6	44	8092.547	0.007	1.2477	a	393.175
21	3	18	21	3	19	8292.111	–0.039	0.7606	a	75.979
30	4	26	30	4	27	8345.508	–0.052	0.9325	a	151.184
47	10	38	48	9	39	8755.744	0.032	7.4591	b	412.596
1	0	1	0	0	0	8904.683	0.003	1.0000	a	0.297
13	2	11	13	2	12	9134.949	–0.030	0.5500	a	30.375
24	4	20	23	5	19	9292.286	0.016	3.7964	b	101.741
40	5	35	40	5	36	9523.942	–0.012	1.0653	a	264.043
50	9	42	49	10	39	9595.237	–0.009	7.8849	b	441.762
50	9	41	49	10	40	9598.753	–0.006	7.8850	b	441.762
60	7	53	60	7	54	9831.807	–0.034	1.3465	a	583.464
21	5	17	22	4	18	9847.631	–0.010	3.3706	b	88.030
6	1	5	6	1	6	9968.495	–0.005	0.3103	a	7.173
50	6	44	50	6	45	9985.912	0.013	1.2038	a	408.170
16	4	12	17	3	15	10125.809	–0.001	2.5800	b	52.820
31	4	27	31	4	28	10523.974	–0.005	0.8865	a	160.504
22	3	19	22	3	20	10631.182	0.000	0.7129	a	82.604
21	5	16	22	4	19	10689.657	0.012	3.3662	b	88.031
11	3	8	12	2	11	11000.105	–0.002	1.7678	b	26.590
45	8	38	44	9	35	11342.344	–0.002	7.1100	b	357.341
45	8	37	44	9	36	11356.180	–0.016	7.1101	b	357.341
26	6	21	27	5	22	11602.414	0.006	4.1457	b	132.218
41	5	36	41	5	37	11799.156	0.004	1.0209	a	276.372
26	6	20	27	5	23	11849.255	–0.009	4.1447	b	132.218
14	2	12	14	2	13	11887.289	0.011	0.5025	a	34.607
51	6	45	51	6	46	12234.502	0.016	1.1601	a	423.475
19	3	16	18	4	15	12539.047	–0.014	3.0304	b	63.658
15	2	14	14	3	11	12699.180	0.004	2.2745	b	38.643
12	1	12	11	2	9	12971.981	–0.004	1.1927	b	23.269
40	7	34	39	8	31	13011.395	–0.001	6.3344	b	281.864
40	7	33	39	8	32	13064.292	–0.066	6.3345	b	281.865
32	4	28	32	4	29	13120.933	–0.005	0.8420	a	170.135
31	7	25	32	6	26	13167.294	0.018	4.9209	b	185.377
7	1	6	7	1	7	13283.439	0.011	0.2690	a	9.305
23	3	20	23	3	21	13418.017	0.005	0.6682	a	89.540
4	0	4	3	1	3	13755.208	0.001	1.6155	b	2.967
23	1	23	22	2	20	14207.170	–0.003	0.4415	b	80.005
10	3	8	11	2	9	14217.930	–0.002	1.6205	b	23.311
42	5	37	42	5	38	14490.223	–0.007	0.9773	a	288.992
35	6	30	34	7	27	14580.891	–0.011	5.5574	b	215.336
36	8	28	37	7	31	14724.127	–0.031	5.6958	b	247.542
35	6	29	34	7	28	14776.125	0.002	5.5582	b	215.343
15	2	13	15	2	14	15118.989	0.015	0.4609	a	39.147
30	5	26	29	6	23	15953.290	0.012	4.7777	b	157.764
33	4	29	33	4	30	16178.439	–0.026	0.7989	a	180.079
24	3	21	24	3	22	16686.715	–0.018	0.6263	a	96.787
8	1	7	8	1	8	17063.758	0.004	0.2379	a	11.739
15	4	12	16	3	13	17193.716	0.008	2.3803	b	48.055
2	1	2	1	1	1	17334.420	0.003	1.5000	a	1.641
2	0	2	1	0	1	17802.003	0.015	1.9998	a	0.891
51	9	43	50	10	40	18802.099	0.000	8.0958	b	456.938
51	9	42	50	10	41	18807.078	0.017	8.0958	b	456.938
2	1	1	1	1	0	18284.549	0.007	1.5000	a	1.688
16	2	14	16	2	15	18843.906	0.026	0.4242	a	43.996
43	3	40	44	2	43	18960.355	0.003	0.4660	b	292.510
15	4	11	16	3	14	19053.454	–0.005	2.3683	b	48.056
25	4	21	24	5	20	19062.862	0.006	4.0049	b	109.215
20	5	16	21	4	17	19256.527	–0.005	3.1539	b	81.778
10	3	7	11	2	10	19308.140	–0.009	1.5691	b	23.314
14	1	14	13	2	11	19715.201	0.001	1.1027	b	31.032
39	2	38	38	3	35	19731.494	0.076	0.6349	b	231.255
34	4	30	34	4	31	19734.187	–0.014	0.7574	a	190.336
20	5	15	21	4	18	19843.158	0.016	3.1511	b	81.778
16	2	15	15	3	12	20057.709	0.014	2.4020	b	43.368
21	1	21	20	2	18	20334.386	–0.005	0.5553	b	67.144

Table 5. continued.

Transition						Obs. Freq.	obs.- calc	S	Dipole	E_u
J'	K'_a	K'_c	J''	K''_a	K''_c	(MHz)	(MHz)			(cm^{-1})
25	3	22	25	3	23	20464.122	0.002	0.5872	a	104.346
46	8	39	45	9	36	20598.708	0.021	7.3202	b	371.039
46	8	38	45	9	37	20618.183	0.017	7.3202	b	371.039
9	1	8	8	2	7	20873.090	–0.019	1.8425	b	14.475
25	6	20	26	5	21	20891.907	0.012	3.9294	b	124.478
25	6	19	26	5	22	21062.686	0.020	3.9287	b	124.478
9	1	8	9	1	9	21303.467	0.041	0.2137	a	14.475
5	2	3	6	1	6	21445.733	0.010	0.7302	b	7.556
4	2	3	5	1	4	21505.270	0.021	0.6445	b	6.063
54	6	48	54	6	49	21554.477	0.030	1.0311	a	471.265
15	1	15	14	2	12	22018.368	0.000	1.0309	b	35.341
41	7	35	40	8	32	22313.417	–0.002	6.5435	b	294.080
41	7	34	40	8	33	22387.468	–0.007	6.5438	b	294.082
30	7	24	31	6	25	22401.921	0.016	4.7048	b	176.150
20	1	20	19	2	17	22415.419	–0.005	0.6234	b	61.137
30	7	23	31	6	26	22449.165	0.061	4.7046	b	176.150
20	3	17	19	4	16	22927.270	0.059	3.2429	b	69.664
17	2	15	17	2	16	23067.910	0.012	0.3920	a	49.153
1	1	0	1	0	1	23420.143	–0.023	1.5000	b	1.073
29	2	27	30	1	30	23440.092	0.021	0.2271	b	134.663
5	0	5	4	1	4	23477.750	0.011	2.2149	b	4.447
16	1	16	15	2	13	23581.913	0.004	0.9495	b	39.934
19	1	19	18	2	16	23801.020	0.007	0.6985	b	55.412
35	4	31	35	4	32	23819.727	0.015	0.7176	a	200.907
2	1	1	2	0	2	23902.727	0.008	2.4743	b	1.688
35	8	28	36	7	29	23904.119	0.028	5.4797	b	236.789
36	6	31	35	7	28	23914.598	–0.002	5.7650	b	226.069
35	8	27	36	7	30	23916.656	0.008	5.4797	b	236.789
36	6	30	35	7	29	24185.405	0.012	5.7662	b	226.078
9	3	7	10	2	8	24209.701	–0.008	1.3908	b	20.336
17	1	17	16	2	14	24397.839	0.008	0.8642	b	44.810
18	1	18	17	2	15	24467.562	–0.005	0.7795	b	49.970
3	1	2	3	0	3	24640.166	0.017	3.4099	b	2.603
26	3	23	26	3	24	24768.720	–0.007	0.5508	a	112.216
21	3	19	20	4	16	24920.535	0.011	3.3551	b	75.703
31	5	27	30	6	24	25269.552	0.001	4.9825	b	167.011
45	5	40	45	5	41	25480.581	0.017	0.8512	a	328.763
4	1	3	4	0	4	25648.624	0.023	4.2915	b	3.822
55	6	49	55	6	50	25661.570	0.017	0.9890	a	487.823
26	4	23	25	5	20	25959.990	0.004	4.1883	b	116.898
10	1	9	10	1	10	25993.978	0.028	0.1944	a	17.514
3	1	3	2	1	2	25996.967	0.008	2.6666	a	2.508
3	0	3	2	0	2	26684.580	0.015	2.9994	a	1.781
3	2	2	2	2	1	26714.950*	0.052	1.6667	a	4.875
3	2	1	2	2	0	26744.010*	–0.073	1.6667	a	4.876
1	1	1	0	0	0	31849.760*	–0.008	1.0000	b	1.062
2	1	2	1	0	1	40279.490*	–0.014	1.5000	b	1.641
29	1	28	28	1	27	255185.831	0.020	28.8310	a	130.821
30	1	29	29	2	28	255697.527	–0.006	18.1072	b	139.610
30	0	30	29	1	29	255729.170	0.024	26.1978	b	133.872
28	2	27	27	1	26	256108.672	0.040	16.1246	b	122.617
30	1	30	29	0	29	256363.437	0.018	26.2016	b	133.881
29	13	17	28	13	16	258615.908	0.011	23.1730	a	259.587
29	8	22	28	8	21	258620.475	0.021	26.7938	a	178.773
29	15	15	28	15	14	258724.290	0.002	21.2419	a	302.554
29	7	22	28	7	21	258726.010	–0.097	27.3109	a	167.222
29	16	13	28	16	12	258792.256	–0.012	20.1730	a	326.294
29	17	12	28	17	11	258868.168	–0.031	19.0350	a	351.528
29	6	24	28	6	23	258918.306	0.019	27.7590	a	157.231
29	6	23	28	6	22	258925.441	0.004	27.7590	a	157.232
29	4	26	28	4	25	259360.975	0.010	28.4442	a	141.956
29	5	24	28	5	23	259365.476	0.026	28.1377	a	148.833
29	23	7	28	23	6	259464.000	–0.044	10.7589	a	533.922
16	2	14	15	1	15	259474.045	0.032	1.3800	b	43.996
29	24	6	28	24	5	259584.036	–0.020	9.1382	a	569.411
29	25	5	28	25	4	259709.560	0.071	7.4485	a	606.332

Table 5. continued.

Transition						Obs. Freq.	obs.- calc	S	Dipole	E_u
J'	K'_a	K'_c	J''	K''_a	K''_c	(MHz)	(MHz)			(cm^{-1})
11	4	7	10	3	8	260134.456	–0.066	4.6036	b	31.988
18	3	16	17	2	15	260458.459	0.083	5.2577	b	57.841
29	4	25	28	4	24	260836.767	0.007	28.4473	a	142.174
6	5	2	5	4	1	261899.605	–0.019	4.5656	b	25.561
30	2	29	29	2	28	262249.715	0.037	29.8108	a	139.829
29	2	27	28	2	26	262526.003	0.030	28.8205	a	134.663
30	1	29	29	1	28	263498.111	0.041	29.8274	a	139.610
29	3	26	28	3	25	263873.574	0.029	28.7082	a	137.692
31	1	31	30	1	30	264425.904	0.015	30.9328	a	142.702
31	0	31	30	0	30	264483.887	0.020	30.9332	a	142.694
50	7	43	50	6	44	280981.325	0.064	28.8964	b	417.542
49	7	42	49	6	43	283184.500	0.045	28.1365	b	402.621
48	7	41	48	6	42	285153.875	0.027	27.3917	b	388.001
47	7	40	47	6	41	286910.300	–0.038	26.6603	b	373.682
46	4	42	45	5	41	293390.100	–0.008	9.3645	b	337.699
39	7	32	39	6	33	295539.200	0.001	21.1602	b	269.948
33	26	8	32	26	7	295594.699	0.030	12.5155	a	682.326
36	2	34	35	3	33	296157.460	–0.009	15.3342	b	203.922
39	7	33	39	6	34	296158.723	–0.003	21.1520	b	269.947
38	7	31	38	6	32	296161.470	–0.024	20.5074	b	258.330
38	7	32	38	6	33	296623.735	–0.037	20.5015	b	258.329
37	7	31	37	6	32	297059.724	–0.025	19.8568	b	247.011
36	7	29	36	6	30	297216.001	–0.025	19.2206	b	235.992
36	7	30	36	6	31	297466.121	–0.045	19.2177	b	235.992
35	7	28	35	6	29	297661.695	–0.050	18.5859	b	225.271
35	7	29	35	6	30	297842.960	–0.026	18.5839	b	225.271
35	0	35	34	1	34	297978.806	–0.015	31.2465	b	180.785
32	7	26	32	6	27	298800.700	–0.057	16.7126	b	194.903
19	3	16	18	2	17	298801.250	–0.074	4.1435	b	63.658
31	7	24	31	6	25	299020.700	–0.048	16.0985	b	185.377
31	7	25	31	6	26	299065.300	–0.071	9.9005	b	185.377
47	4	43	46	5	42	309438.250	–0.025	36.2762	b	351.962
40	0	40	39	1	39	340045.815	–0.013	36.2764	b	234.704
40	1	40	39	0	39	340105.443	–0.023	36.2764	b	234.705
48	8	41	48	7	42	340202.976	–0.018	26.3427	b	399.329
47	8	39	47	7	40	340359.169	0.007	25.6798	b	385.035
40	2	38	39	3	37	340405.369	–0.008	19.7751	b	249.619
47	8	40	47	7	41	340778.017	0.094	25.6749	b	385.034
20	4	16	19	3	17	340964.440	–0.076	6.0477	b	74.872
46	8	38	46	7	39	341004.519	0.018	25.0163	b	371.039
49	4	45	48	5	44	341521.050	–0.019	11.1390	b	381.371
15	5	11	14	4	10	341931.393	–0.009	6.0859	b	54.997
15	5	10	14	4	11	341956.342	0.099	6.0857	b	54.997
21	4	18	20	3	17	343330.662	–0.058	6.2876	b	81.117
12	8	4	12	7	5	346872.475*	–0.115	4.0659	b	72.603
41	0	41	40	1	40	348447.304	–0.014	37.2806	b	246.328
41	1	41	40	1	40	348467.894	–0.001	40.9323	a	246.328
41	0	41	40	0	40	348473.530	–0.018	40.9323	a	246.328
41	1	41	40	0	40	348494.137	0.012	37.2808	b	246.328
39	6	34	38	6	33	348749.756	0.027	38.0771	a	260.068
39	6	33	38	6	32	348917.871	0.026	38.0773	a	260.090
39	5	35	38	5	34	349107.718	0.012	38.3554	a	251.782
37	3	35	36	2	34	349598.675	0.065	16.7661	b	215.583
22	4	19	21	3	18	350598.197	0.025	6.4294	b	87.674
39	5	34	38	5	33	350685.690	0.022	38.3590	a	252.036
41	2	39	40	3	38	350753.900	–0.009	20.8971	b	261.732
16	5	11	15	4	12	350810.905	0.042	6.2710	b	59.756
11	6	6	10	5	5	352675.302	–0.088	6.1011	b	47.431
40	3	38	39	3	37	352770.932	0.008	39.7036	a	250.032
39	3	36	38	3	35	354017.727	0.073	38.7486	a	242.405
41	1	40	40	2	39	354334.508	0.031	29.6761	b	254.638
39	4	35	38	4	34	354433.785	0.004	38.6153	a	246.321
40	2	38	39	2	37	354874.352	0.004	39.7314	a	249.619
41	2	40	40	2	39	355087.351	0.015	40.8103	a	254.638
38	3	36	37	2	35	355214.666	0.068	17.8152	b	226.782
40	12	29	39	12	28	356545.046	0.016	36.4011	a	354.859

Table 5. continued.

Transition						Obs. Freq.	obs.- calc	S	Dipole	E_u
J'	K'_a	K'_c	J''	K''_a	K''_c	(MHz)	(MHz)			(cm^{-1})
40	14	26	39	14	25	356597.850	–0.005	35.1010	a	394.831
40	9	32	39	9	31	356729.510	0.072	37.9761	a	306.388
40	17	23	39	17	22	356818.075	–0.092	32.7759	a	466.122
42	0	42	41	1	41	356845.808	–0.016	38.2847	b	258.231
42	1	42	41	1	41	356861.934	–0.020	41.9323	a	258.232
42	0	42	41	0	41	356866.384	–0.017	41.9323	a	258.231
42	1	42	41	0	41	356882.504	–0.027	38.2849	b	258.232
50	4	46	49	5	45	357454.500	–0.023	11.8467	b	396.513
23	4	20	22	3	19	357550.155	–0.057	6.5689	b	94.531
40	27	14	39	27	13	358265.947	–0.070	21.7756	a	799.501

Table 6. Sample table of the predicted transitions of the ground vibrational state of $^{13}CH_3CH_2CN$. The entire table is available in electronic form on the CDS.

Transition J' (K_a', K_c')–J'' (K_a'', K_c'')	Calc. Frequency (MHz)	Exp. Error (MHz)	S	Dipole	E_l cm^{-1}
3 (1, 3)–2 (1, 2)	25494.7	0.03	2.6666	A	1.62
3 (0, 3)–2 (0, 2)	26166.99	0.03	2.9994	A	0.87
3 (2, 2)–2 (2, 1)	26196.27	0.03	1.6667	A	3.94
3 (2, 1)–2 (2, 0)	26224.4	0.03	1.6667	A	3.94
3 (1, 2)–2 (1, 1)	26887.32	0.03	2.6666	A	1.66
8 (1, 7)–8 (0, 8)	32434.75	0.03	7.0176	B	10.44
4 (1, 4)–3 (1, 3)	33984.63	0.03	3.7498	A	2.47
4 (0, 4)–3 (0, 3)	34856.26	0.03	3.9985	A	1.75
4 (2, 3)–3 (2, 2)	34922.57	0.03	2.9999	A	4.81
4 (3, 2)–3 (3, 1)	34943.83	0.03	1.75	A	8.64
4 (3, 1)–3 (3, 0)	34944.22	0.03	1.75	A	8.64
4 (2, 2)–3 (2, 1)	34992.79	0.03	2.9999	A	4.81
9 (1, 8)–9 (0, 9)	35118.09	0.03	7.4437	B	13.03
4 (1, 3)–3 (1, 2)	35840.99	0.03	3.7498	A	2.56
10 (1, 9)–10 (0, 10)	38229.04	0.03	7.7595	B	15.91
11 (1, 10)–11 (0, 11)	41792.14	0.03	7.9693	B	19.06
7 (0, 7)–6 (1, 6)	42238.57	0.03	3.537	B	6.72
5 (1, 5)–4 (1, 4)	42467.64	0.03	4.7995	A	3.60
5 (0, 5)–4 (0, 4)	43517.43	0.03	4.997	A	2.91
5 (2, 4)–4 (2, 3)	43643.89	0.03	4.1998	A	5.98
5 (4, 2)–4 (4, 1)	43680.91	0.03	1.8	A	15.17
5 (4, 1)–4 (4, 0)	43680.91	0.03	1.8	A	15.17
5 (3, 3)–4 (3, 2)	43685.39	0.03	3.2	A	9.81
5 (3, 2)–4 (3, 1)	43686.79	0.03	3.2	A	9.81
5 (2, 3)–4 (2, 2)	43784.02	0.03	4.1998	A	5.98
5 (1, 4)–4 (1, 3)	44786.95	0.03	4.7995	A	3.76
12 (1, 11)–12 (0, 12)	45824.96	0.03	8.0828	B	22.50
17 (2, 15)–16 (3, 14)	49527.68	0.04	3.0925	B	46.57
29 (4, 26)–28 (5, 23)	49951.78	0.19	4.7505	B	137.66
13 (1, 12)–13 (0, 13)	50335.88	0.03	8.114	B	26.21
6 (1, 6)–5 (1, 5)	50942.25	0.03	5.8325	A	5.02
34 (5, 29)–33 (6, 28)	51608.89	0.57	5.5932	B	191.28
8 (0, 8)–7 (1, 7)	52102.75	0.03	4.2734	B	8.70
6 (0, 6)–5 (0, 5)	52144.02	0.03	5.9948	A	4.36
6 (2, 5)–5 (2, 4)	52359.02	0.03	5.3329	A	7.43
6 (5, 2)–5 (5, 1)	52420.32	0.03	1.8334	A	23.52
6 (5, 1)–5 (5, 0)	52420.32	0.03	1.8334	A	23.52
6 (4, 3)–5 (4, 2)	52421.45	0.03	3.3334	A	16.63
6 (4, 2)–5 (4, 1)	52421.47	0.03	3.3334	A	16.63
6 (3, 4)–5 (3, 3)	52430.34	0.03	4.5001	A	11.27
6 (3, 3)–5 (3, 2)	52434.07	0.03	4.5001	A	11.27
6 (2, 4)–5 (2, 3)	52603.27	0.03	5.333	A	7.44
12 (1, 11)–11 (2, 10)	52789.21	0.03	2.9911	B	22.26
23 (3, 20)–22 (4, 19)	52853.92	0.04	3.8771	B	86.10
6 (1, 5)–5 (1, 4)	53723.03	0.03	5.8324	A	5.25
25 (3, 23)–24 (4, 20)	54973.12	0.03	3.9388	B	99.89
14 (1, 13)–14 (0, 14)	55322.5	0.03	8.08	B	30.19
4 (1, 4)–3 (0, 3)	55599.48	0.03	2.5378	B	1.75
29 (4, 25)–28 (5, 24)	56423.08	0.3	4.81	B	137.65
40 (6, 35)–39 (7, 32)	57043.19	1.18	6.5739	B	265.10
14 (2, 12)–14 (1, 13)	57651.29	0.03	11.3523	B	32.04
13 (2, 11)–13 (1, 12)	57800.41	0.03	10.2992	B	27.89
15 (2, 13)–15 (1, 14)	57862.46	0.04	12.3609	B	36.48
40 (6, 34)–39 (7, 33)	57874.83	1.27	6.5781	B	265.10
12 (2, 10)–12 (1, 11)	58264.01	0.03	9.2292	B	24.02
16 (2, 14)–16 (1, 15)	58474.85	0.04	13.298	B	41.22
35 (5, 31)–34 (6, 28)	58679.67	0.56	5.7682	B	201.22
...					

Table 7. Sample table of the predicted transitions of the ground vibrational state of $CH_3^{13}CH_2CN$. The entire table is available in electronic form on the CDS.

Transition J' (K'_a, K'_c)–J'' (K''_a, K''_c)	Calc. Frequency (MHz)	Exp. Error (MHz)	S	Dipole	E_l cm^{-1}
25 (4, 21)–24 (5, 20)	25052.91	0.14	3.9927	B	108.11
4 (1, 3)–4 (0, 4)	25145.98	0.04	4.2789	B	2.97
3 (1, 3)–2 (1, 2)	25974.04	0.04	2.6666	A	1.62
44 (5, 39)–44 (5, 40)	26337.74	1.45	0.8626	A	314.10
5 (1, 4)–5 (0, 5)	26496.50	0.04	5.0804	B	4.45
3 (0, 3)–2 (0, 2)	26682.90	0.04	2.9993	A	0.89
3 (2, 2)–2 (2, 1)	26715.94	0.04	1.6667	A	3.91
3 (2, 1)–2 (2, 0)	26747.90	0.04	1.6667	A	3.91
10 (1, 9)–10 (1, 10)	26839.67	0.04	0.1948	A	16.61
3 (1, 2)–2 (1, 1)	27446.24	0.04	2.6666	A	1.67
26 (3, 23)–26 (3, 24)	27803.68	0.1	0.5397	A	111.22
20 (3, 17)–19 (4, 16)	27931.11	0.04	3.2364	B	68.60
54 (6, 48)–54 (6, 49)	27935.99	4.17	0.9907	A	470.04
35 (4, 31)–35 (4, 32)	28021.12	0.51	0.6975	A	199.84
6 (1, 5)–6 (0, 6)	28180	0.04	5.7941	B	6.22
21 (3, 19)–20 (4, 16)	28855.09	0.04	3.3275	B	74.57
17 (2, 16)–16 (3, 13)	29182.38	0.04	2.4486	B	47.32
18 (2, 16)–18 (2, 17)	29803.14	0.04	0.3601	A	53.60
7 (1, 6)–7 (0, 7)	30228.05	0.04	6.4075	B	8.28
51 (9, 43)–50 (10, 40)	30726.21	4.13	8.074	B	454.42
51 (9, 42)–50 (10, 41)	30734.36	4.13	8.0741	B	454.42
8 (3, 6)–9 (2, 7)	30838.26	0.04	1.1632	B	16.45
1 (1, 1)–0 (0, 0)	31252.54	0.04	1	B	0
46 (8, 39)–45 (9, 36)	31286.92	2.47	7.2996	B	368.82
46 (8, 38)–45 (9, 37)	31317.04	2.49	7.2997	B	368.82
45 (5, 40)–45 (5, 41)	31326.09	1.76	0.8208	A	327.53
26 (4, 23)–25 (5, 20)	31440.15	0.12	4.1679	B	115.56
41 (7, 35)–40 (8, 32)	31760.66	1.39	6.5241	B	292.13
13 (4, 10)–14 (3, 11)	31830.81	0.04	1.936	B	38.05
41 (7, 34)–40 (8, 33)	31868.63	1.41	6.5245	B	292.13
36 (6, 31)–35 (7, 28)	32103.27	0.72	5.7465	B	224.35
11 (1, 10)–11 (1, 11)	32128.36	0.04	0.1794	A	19.78
31 (5, 27)–30 (6, 24)	32152.84	0.32	4.9642	B	165.49
18 (5, 14)–19 (4, 15)	32344.14	0.04	2.7116	B	68.61
15 (2, 13)–14 (3, 12)	32472.81	0.04	2.5825	B	38.02
36 (6, 30)–35 (7, 29)	32475.37	0.75	5.7481	B	224.35
23 (6, 18)–24 (5, 19)	32633.60	0.07	3.4871	B	108.11
18 (5, 13)–19 (4, 16)	32674.01	0.04	2.7103	B	68.60
8 (1, 7)–8 (0, 8)	32674.24	0.04	6.9113	B	10.64
23 (6, 17)–24 (5, 20)	32735.07	0.07	3.4868	B	108.11
13 (4, 9)–14 (3, 12)	32824.55	0.04	1.9308	B	38.02
28 (7, 22)–29 (6, 23)	32857.27	0.17	4.262	B	156.55
28 (7, 21)–29 (6, 24)	32886.96	0.17	4.2619	B	156.55
55 (6, 49)–55 (6, 50)	33034.68	5.01	0.9473	A	486.47
33 (8, 26)–34 (7, 27)	33082.89	0.41	5.0362	B	213.92
33 (8, 25)–34 (7, 28)	33091.26	0.41	5.0362	B	213.92
27 (3, 24)–27 (3, 25)	33099.13	0.12	0.5066	A	119.24
36 (4, 32)–36 (4, 33)	33297.29	0.62	0.6595	A	210.57
38 (9, 30)–39 (8, 31)	33339.72	0.85	5.8099	B	280.22
38 (9, 29)–39 (8, 32)	33342.02	0.85	5.8099	B	280.22
31 (5, 26)–30 (6, 25)	33371.50	0.36	4.9708	B	165.49
8 (3, 5)–9 (2, 8)	33444.91	0.04	1.1449	B	16.37
43 (10, 34)–44 (9, 35)	33643.14	1.59	6.583	B	355.43
43 (10, 33)–44 (9, 36)	33643.75	1.59	6.583	B	355.43
48 (11, 38)–49 (10, 39)	34003.63	2.79	7.3557	B	439.55
48 (11, 37)–49 (10, 40)	34003.78	2.79	7.3557	B	439.55
6 (0, 6)–5 (1, 5)	34012.64	0.04	2.8771	B	5.08
...					

Table 8. Sample table of the predicted transitions of the ground vibrational state of $CH_3CH_2^{13}CN$. The entire table is available in electronic form on the CDS.

Transition J' (K_a', K_c')–J'' (K_a'', K_c'')	Calc. Frequency (MHz)	Exp. Error (MHz)	S	Dipole	E_l cm^{-1}
3 (1, 3)–2 (1, 2)	25996.96	0.03	2.6666	A	1.64
3 (0, 3)–2 (0, 2)	26684.57	0.03	2.9994	A	0.89
3 (2, 2)–2 (2, 1)	26714.90	0.03	1.6667	A	3.98
3 (2, 1)–2 (2, 0)	26744.08	0.03	1.6667	A	3.98
3 (1, 2)–2 (1, 1)	27422.00	0.03	2.6666	A	1.69
7 (1, 6)–7 (0, 7)	30532.86	0.03	6.468	B	8.29
8 (1, 7)–8 (0, 8)	32876.36	0.03	6.9975	B	10.64
4 (1, 4)–3 (1, 3)	34654.00	0.03	3.7498	A	2.51
4 (0, 4)–3 (0, 3)	35545.12	0.03	3.9984	A	1.78
4 (2, 3)–3 (2, 2)	35613.85	0.03	2.9999	A	4.88
9 (1, 8)–9 (0, 9)	35629.74	0.03	7.4166	B	13.29
4 (3, 2)–3 (3, 1)	35635.82	0.03	1.75	A	8.74
4 (3, 1)–3 (3, 0)	35636.24	0.03	1.75	A	8.74
4 (2, 2)–3 (2, 1)	35686.73	0.03	2.9999	A	4.88
4 (1, 3)–3 (1, 2)	36553.57	0.03	3.7498	A	2.60
10 (1, 9)–10 (0, 10)	38822.57	0.03	7.7246	B	16.22
11 (1, 10)–11 (0, 11)	42479.70	0.03	7.9265	B	19.44
5 (1, 5)–4 (1, 4)	43303.87	0.03	4.7995	A	3.66
7 (0, 7)–6 (1, 6)	43326.73	0.03	3.5444	B	6.84
5 (0, 5)–4 (0, 4)	44376.53	0.03	4.9969	A	2.97
5 (2, 4)–4 (2, 3)	44507.66	0.03	4.1998	A	6.06
5 (4, 2)–4 (4, 1)	44545.79	0.03	1.8	A	15.34
5 (4, 1)–4 (4, 0)	44545.79	0.03	1.8	A	15.34
5 (3, 3)–4 (3, 2)	44550.60	0.03	3.2001	A	9.93
5 (3, 2)–4 (3, 1)	44552.08	0.03	3.2001	A	9.93
5 (2, 3)–4 (2, 2)	44653.08	0.03	4.1998	A	6.07
5 (1, 4)–4 (1, 3)	45677.15	0.03	4.7995	A	3.82
12 (1, 11)–12 (0, 12)	46618.62	0.03	8.0324	B	22.94
28 (4, 24)–27 (5, 23)	49471.56	0.03	4.6101	B	131.82
24 (3, 22)–23 (4, 19)	49796.81	0.03	3.8082	B	94.57
13 (1, 12)–13 (0, 13)	51247.06	0.03	8.0569	B	26.72
6 (1, 6)–5 (1, 5)	51945.04	0.03	5.8325	A	5.11
17 (2, 15)–16 (3, 14)	51955.10	0.03	3.0976	B	47.42
6 (0, 6)–5 (0, 5)	53172.09	0.03	5.9946	A	4.45
29 (4, 26)–28 (5, 23)	53185.48	0.03	4.7418	B	140.18
34 (5, 30)–33 (6, 27)	53311.67	0.03	5.573	B	194.77
8 (0, 8)–7 (1, 7)	53383.42	0.03	4.2838	B	8.86
6 (2, 5)–5 (2, 4)	53395.05	0.03	5.3329	A	7.55
6 (5, 2)–5 (5, 1)	53458.07	0.03	1.8334	A	23.78
6 (5, 1)–5 (5, 0)	53458.07	0.03	1.8334	A	23.78
6 (4, 3)–5 (4, 2)	53459.50	0.03	3.3334	A	16.82
6 (4, 2)–5 (4, 1)	53459.52	0.03	3.3334	A	16.82
6 (3, 4)–5 (3, 3)	53468.90	0.03	4.5001	A	11.42
6 (3, 3)–5 (3, 2)	53472.82	0.03	4.5001	A	11.42
6 (2, 4)–5 (2, 3)	53648.47	0.03	5.333	A	7.56
12 (1, 11)–11 (2, 10)	54621.10	0.03	3.0024	B	22.67
6 (1, 5)–5 (1, 4)	54790.46	0.03	5.8324	A	5.35
34 (5, 29)–33 (6, 28)	55582.99	0.03	5.5872	B	194.77
23 (3, 20)–22 (4, 19)	55941.87	0.03	3.8759	B	87.67
14 (1, 13)–14 (0, 14)	56361.47	0.03	8.0174	B	30.79
4 (1, 4)–3 (0, 3)	56443.91	0.03	2.5383	B	1.78
21 (6, 16)–22 (5, 17)	57611.90	0.03	3.0489	B	94.58
25 (3, 23)–24 (4, 20)	57640.40	0.03	3.922	B	101.74
21 (6, 15)–22 (5, 18)	57645.00	0.03	3.0488	B	94.58
14 (2, 12)–14 (1, 13)	58171.43	0.03	11.3774	B	32.67
13 (2, 11)–13 (1, 12)	58288.93	0.03	10.3273	B	28.43
15 (2, 13)–15 (1, 14)	58427.15	0.03	12.3798	B	37.20
...					

Table 9. Emission lines of $CH_3CH_2^{13}CN$ (without high blend) present in the frequency range of the Orion KL survey. Column 1 indicates the transition, Col. 2 gives the calculated frequencies, Col. 3 gives the line strenght, Col. 4 the energy of the upper level, Col. 5 the observed (centroid)frequencies assuming that the radial velocities relative to LSR are 5 km s^{-1}, Col. 6 the observed temperature of main beam and Col. 7 gives the main beam temperature obtained with the model.

Transitions J_{K_a,K_c}	Predicted Frequency	S_{ij}	E_u/k (K)	Observed Frequency	Observed $T_{\rm mb}$ (K)	Model $T_{\rm mb}$ (K)
$9_{1,8}$–$8_{1,7}$	80447.460	8.89	20.4	80447.4	0.030	0.019
$10_{2,9}$–$9_{2,8}$	87133.148	9.60	27.4	87132.3	0.041	0.024
$10_{6,5}$–$9_{6,4}$	87386.059	6.40	62.7	87386.2	0.039	0.031
$10_{6,4}$–$9_{6,3}$	87386.059	6.40	62.7	[1]		
$10_{7,4}$–$9_{7,3}$	87389.467	5.10	77.0	87389.2	0.073	0.044
$10_{7,3}$–$9_{7,2}$	87389.467	5.10	77.0	[1]		
$10_{5,6}$–$9_{5,5}$	87390.833	7.50	50.6	[1]		
$10_{5,5}$–$9_{5,4}$	87390.840	7.50	50.6	[1]		
$10_{9,2}$–$9_{9,1}$	87410.354	1.90	112.2	87410.2	0.060	0.037
$10_{9,1}$–$9_{9,0}$	87410.354	1.90	112.2	[1]		
$10_{4,7}$–$9_{4,6}$	87411.059	8.40	40.7	[1]		
$10_{4,6}$–$9_{4,5}$	87411.951	8.40	40.7	[1]		
$10_{2,8}$–$9_{2,7}$	88230.982	9.60	27.6	88231.2	0.028	0.025
$11_{1,11}$–$10_{1,10}$	93149.851	10.9	28.0	93150.2	0.056[2]	0.033
$11_{0,11}$–$10_{0,10}$	94602.308	11.0	27.4	94602.2	0.020	0.035
$11_{2,10}$–$10_{2,9}$	95799.141	10.6	32.0	95799.2	0.034	0.035
$11_{6,6}$–$10_{6,5}$	96129.640	7.73	67.3	96132.2	0.031	0.053
$11_{6,5}$–$10_{6,4}$	96129.640	7.73	67.3	[1]		
$11_{7,5}$–$10_{7,4}$	96131.299	6.55	81.7	[1]		
$11_{7,4}$–$10_{7,3}$	96131.299	6.55	81.7	[1]		
$11_{5,7}$–$10_{5,6}$	96138.428	8.73	55.2	96138.3	0.49	0.069
$11_{5,6}$–$10_{5,5}$	96138.446	8.73	55.2	[1]		
$11_{8,4}$–$10_{8,3}$	96139.380	5.18	98.2	[1]		
$11_{8,3}$–$10_{8,2}$	96139.380	5.18	98.2	[1]		
$11_{9,2}$–$10_{9,1}$	96152.023	3.64	116.8	96152.2	0.015	0.017
$11_{9,3}$–$10_{9,2}$	96152.023	3.64	116.8	[1]		
$11_{10,1}$–$10_{10,0}$	96168.265	1.91	137.7	96169.2	0.036	0.045
$11_{10,2}$–$10_{10,1}$	96168.265	1.91	137.7	[1]		
$11_{4,7}$–$10_{4,6}$	96168.855	9.55	45.3	[1]		
$11_{3,9}$–$10_{3,8}$	96210.322	10.2	37.6	96209.2	0.041	0.033
$11_{3,8}$–$10_{3,7}$	96294.719	10.2	37.6	96294.2	0.033	0.033
$11_{2,9}$–$10_{2,8}$	97229.062	10.6	32.3	97229.2	0.028	0.036
$11_{1,10}$–$10_{1,9}$	98165.400	10.9	29.4	98165.2	0.049	0.039
$12_{1,12}$–$11_{1,11}$	101553.324	11.9	32.8	101553.1	0.038	0.046
$12_{0,12}$–$11_{0,11}$	102952.092	12.0	32.4	102951.3	0.042	0.047
$12_{7,6}$–$11_{7,5}$	104873.951	7.92	86.7	104874.0	0.099	0.110
$12_{7,5}$–$11_{7,4}$	104873.951	7.92	86.7	[1]		
$12_{6,7}$–$11_{6,6}$	104874.638	9.00	72.4	[1]		
$12_{6,6}$–$11_{6,5}$	104874.638	9.00	72.4	[1]		
$12_{8,5}$–$11_{8,4}$	104881.167	6.67	103.2	104881.1	0.055	0.045
$12_{8,4}$–$11_{8,3}$	104881.167	6.67	103.2	[1]		
$12_{5,8}$–$11_{5,7}$	104888.446	9.92	60.3	104888.1	0.093	0.077
$12_{5,7}$–$11_{5,6}$	104888.488	9.92	60.3	[1]		
$12_{9,4}$–$11_{9,3}$	104893.870	5.25	121.9	104892.1	0.053	0.035
$12_{9,3}$–$11_{9,2}$	104893.870	5.25	121.9	[1]		
$12_{10,3}$–$11_{10,2}$	104910.813	3.67	142.7	104911.1	0.051[3]	0.020
$12_{10,2}$–$11_{10,1}$	104910.813	3.67	142.7	[1]		
$12_{4,9}$–$11_{4,8}$	104927.146	10.7	50.4	104927.1	0.067	0.047
$12_{4,8}$–$11_{4,7}$	104930.478	10.7	50.4	104930.1	0.071	0.054
$12_{11,1}$–$11_{11,0}$	104931.294	1.92	165.8	[1]		
$12_{11,2}$–$11_{11,1}$	104931.294	1.92	165.8	[1]		
$12_{3,9}$–$11_{3,8}$	105105.880	11.2	42.7	105106.1	0.047	0.046
$12_{2,10}$–$11_{2,9}$	106257.491	11.7	37.4	106257.1	0.059	0.050
$12_{1,11}$–$11_{1,10}$	106984.906	11.9	34.6	106986.0	0.089[3]	0.052
$13_{1,13}$–$12_{1,12}$	109943.507	12.9	38.1	109944.0	0.077	0.061
$13_{0,13}$–$12_{0,12}$	111262.117	13.0	37.7	111263.0	0.050	0.062
$13_{2,12}$–$12_{2,11}$	113090.192	12.7	42.5	113090.0	0.095	0.063
$13_{7,7}$–$12_{7,6}$	113617.495	9.23	92.1	113617.5	0.110	0.086
$13_{7,6}$–$12_{7,5}$	113617.495	9.23	92.1	[1]		
$13_{6,8}$–$12_{6,7}$	113621.178	10.2	77.8	113623.0	0.186[3]	0.099
$13_{6,7}$–$12_{6,6}$	113621.179	10.2	77.8	[1]		
$13_{8,6}$–$12_{8,5}$	113623.430	8.08	108.6	[1]		

Table 9. continued.

Transitions J_{K_a,K_c}	predicted Frequency	S_{ij}	E_u/k (K)	Observed Frequency	Observed T_{mb} (K)	Model T_{mb} (K)
$13_{8,5}-12_{8,4}$	113623.430	8.08	108.6	[1]		
$13_{5,9}-12_{5,8}$	113641.101	11.1	65.7	113643.0	0.121[4]	0.104
$13_{5,8}-12_{5,7}$	113641.191	11.1	65.7	[1]		
$13_{4,10}-12_{4,9}$	113691.511	11.8	55.8	113693.0	0.125[3]	0.058
$13_{4,9}-12_{4,8}$	113697.418	11.8	55.8	113695.0	0.148[3]	0.060
$15_{2,14}-14_{2,13}$	130319.914	14.7	54.6	130319.7	0.127	0.102
$15_{7,9}-14_{7,8}$	131107.549	11.7	104.3	131107.2	0.116	0.169
$15_{7,8}-14_{7,7}$	131107.549	11.7	104.3	[1]		
$15_{8,8}-14_{8,7}$	131109.535	10.7	120.8	[1]		
$15_{8,7}-14_{8,6}$	131109.535	10.7	120.8	[1]		
$15_{6,10}-14_{6,9}$	131119.392	12.6	90.0	131119.6	0.134	0.217
$15_{6,9}-14_{6,8}$	131119.396	12.6	90.0	[1]		
$15_{9,6}-14_{9,5}$	131120.630	9.60	139.5	[1]		
$15_{9,7}-14_{9,4}$	131120.630	9.60	139.5	[1]		
$15_{5,11}-14_{5,10}$	131155.172	13.3	77.9	131155.9	0.113	0.172
$15_{5,10}-14_{5,9}$	131155.510	13.3	77.9	[1]		
$15_{4,12}-14_{4,11}$	131233.743	13.9	68.0	131234.6	0.175	0.093
$15_{3,12}-14_{3,11}$	131665.685	14.4	60.3	131666.8	0.173	0.100
$15_{1,14}-14_{1,13}$	133238.773	14.9	52.5	133238.4	0.122	0.112
$15_{2,13}-14_{2,12}$	133449.945	14.7	55.3	133449.6	0.113	0.110
$16_{0,16}-15_{0,15}$	136023.425	15.9	56.1	136024.7	0.261[5]	0.121
$16_{8,9}-15_{8,8}$	139853.452	12.0	127.5	139853.6	0.346	0.310
$16_{8,8}-15_{8,7}$	139853.452	12.0	127.5	[1]		
$16_{7,10}-15_{7,9}$	139854.203	12.9	111.0	[1]		
$16_{7,9}-15_{7,8}$	139854.203	12.9	111.0	[1]		
$16_{11,5}-15_{11,4}$	139904.511	8.44	190.1	139905.6	0.157	0.085
$16_{11,6}-15_{11,5}$	139904.511	8.44	190.1	[1]		
$16_{5,12}-15_{5,11}$	139916.999	14.4	84.6	139917.7	0.256	0.209
$16_{5,11}-15_{5,10}$	139917.612	14.4	84.6	[1]		
$16_{4,13}-15_{4,12}$	140011.723	15.0	74.7	140010.8	0.171	0.172
$16_{3,13}-15_{3,12}$	140571.440	15.4	67.1	140570.6	0.150	0.125
$16_{1,15}-15_{1,14}$	141908.026	15.9	59.3	141907.6	0.283[3]	0.135
$16_{2,14}-15_{2,13}$	142520.417	15.8	62.1	142520.7	0.173	0.143
$17_{0,17}-16_{0,16}$	144244.475	16.9	63.0	144243.2	0.367[6]	0.150
$17_{9,9}-16_{9,8}$	148606.294	12.2	153.3	148607.5	0.242	0.191
$17_{9,8}-16_{9,7}$	148606.294	12.2	153.3	[1]		
$17_{10,7}-16_{10,6}$	148623.395	11.1	174.2	148625.5	0.520[3]	0.292
$17_{10,8}-16_{10,7}$	148623.395	11.1	174.2	[1]		
$17_{6,12}-16_{6,11}$	148625.291	14.9	103.8	[1]		
$17_{6,11}-16_{6,10}$	148625.308	14.9	103.8	[1]		
$17_{11,6}-16_{11,5}$	148647.317	9.88	197.3	148646.5	0.178[6]	0.114
$17_{11,7}-16_{11,6}$	148647.317	9.88	197.3	[1]		
$17_{5,13}-16_{5,12}$	148682.284	15.5	91.7	148682.5	0.592[3]	0.244
$17_{5,12}-16_{5,11}$	148683.353	15.5	91.7	[1]		
$17_{4,13}-16_{4,12}$	148833.482	16.1	81.9	148835.5	0.186	0.143
$17_{2,15}-16_{2,14}$	151579.595	16.8	69.4	151580.5	0.387[3]	0.165
$18_{1,18}-17_{1,17}$	151706.789	17.9	70.5	151706.5	0.294	0.176
$18_{0,18}-17_{0,17}$	152458.988	17.9	70.3	152461.8	0.283[7]	0.177
$18_{9,10}-17_{9,9}$	157349.515	13.5	160.9	157349.3	0.521	0.393
$18_{9,9}-17_{9,8}$	157349.515	13.5	160.9	[1]		
$18_{7,12}-17_{7,11}$	157351.120	15.3	125.7	[1]		
$18_{7,11}-17_{7,10}$	157351.120	15.3	125.7	[1]		
$18_{10,9}-17_{10,8}$	157365.862	12.4	181.8	157367.5	0.230	0.177
$18_{10,8}-17_{10,7}$	157365.862	12.4	181.8	[1]		
$18_{6,13}-17_{6,12}$	157381.436	16.0	111.4	157381.7	0.310	0.297
$18_{6,12}-17_{6,11}$	157381.469	16.0	111.4	[1]		
$18_{11,8}-17_{11,7}$	157389.894	11.3	204.8	157389.9	0.238[8]	0.155
$18_{11,7}-17_{11,6}$	157389.894	11.3	204.8	[1]		
$18_{5,14}-17_{5,13}$	157451.213	16.6	99.3	157454.3	0.413	0.251
$18_{5,13}-17_{5,12}$	157453.015	16.6	99.3	[1]		
$18_{13,6}-17_{13,5}$	157455.918	8.61	257.4	[1]		
$18_{13,5}-17_{13,4}$	157455.918	8.61	257.4	[1]		
$18_{3,16}-17_{3,15}$	157547.788	17.5	81.7	157548.0	0.270	0.183
$18_{4,15}-17_{4,14}$	157580.952	17.1	89.4	157581.4	0.249	0.172
$18_{4,14}-17_{4,13}$	157639.476	17.1	89.4	157639.4	0.205	0.173

Table 9. continued.

Transitions J_{K_a,K_c}	predicted Frequency	S_{ij}	E_u/k (K)	Observed Frequency	Observed $T_{\rm mb}$ (K)	Model $T_{\rm mb}$ (K)
$18_{3,15}-17_{3,14}$	158478.787	17.5	81.9	158478.0	0.170	0.183
$18_{1,17}-17_{1,17}$	159100.090	17.9	74.2	159101.8	0.273	0.195
$19_{1,19}-18_{1,18}$	160026.236	18.9	78.2	160026.7	0.508[3]	0.206
$19_{0,19}-18_{0,18}$	160671.057	18.9	78.1	160671.4	0.282[9]	0.209
$19_{8,12}-18_{8,11}$	166089.105	15.6	150.2	166090.4	0.215	0.306
$19_{8,11}-18_{8,10}$	166089.105	15.6	150.2	[1]		
$19_{9,11}-18_{9,10}$	166093.013	14.7	168.9	[1]		
$19_{9,10}-18_{9,9}$	166093.013	14.7	168.9	[1]		
$19_{6,14}-18_{6,13}$	166139.881	17.1	119.4	166139.1	0.247	0.356
$19_{6,13}-18_{6,12}$	166139.941	17.1	119.4	[1]		
$19_{13,6}-18_{13,5}$	166199.966	10.1	265.4	166200.4	0.231[8]	0.124
$19_{13,7}-18_{13,6}$	166199.966	10.1	265.4	[1]		
$19_{14,5}-18_{14,4}$	166242.063	8.68	294.9	166242.9	0.167	0.095
$19_{14,6}-18_{14,5}$	166242.063	8.68	294.9	[1]		
$19_{16,3}-18_{16,2}$	166340.293	5.53	360.4	166340.4	0.093	0.048
$19_{16,4}-18_{16,3}$	166340.293	5.53	360.4	[1]		
$19_{4,16}-18_{4,15}$	166371.655	18.2	97.4	166375.4	0.230[10,11]	0.204
$19_{4,15}-18_{4,14}$	166456.803	18.2	97.4	166456.7	0.151	0.211
$19_{3,16}-18_{3,15}$	167484.077	18.5	89.9	167484.1	0.363[3]	0.218
$19_{1,18}-18_{1,17}$	167617.052	18.9	82.2	167617.2	0.357	0.228
$20_{0,20}-19_{0,19}$	168883.556	19.9	86.2	168884.3	0.204	0.243
$19_{2,17}-18_{2,16}$	169635.277	18.8	85.2	169635.3	0.252	0.232
$20_{8,13}-19_{8,12}$	174835.743	16.8	158.6	174835.2	0.952	0.596
$20_{8,12}-19_{8,11}$	174835.743	16.8	158.6	[1]		
$20_{9,12}-19_{9,11}$	174836.800	16.0	177.3	[1]		
$20_{9,11}-19_{9,10}$	174836.800	16.0	177.3	[1]		
$20_{11,9}-19_{11,8}$	174874.303	14.0	221.2	174874.2	0.495	0.226
$20_{11,10}-19_{11,9}$	174874.303	14.0	221.2	[1]		
$20_{6,15}-19_{6,14}$	174900.750	18.2	127.8	174901.1	0.847[12]	0.421
$20_{6,14}-19_{6,13}$	174900.857	18.2	127.8	[1]		
$20_{12,9}-19_{12,8}$	174905.610	12.8	246.4	[1]		
$20_{12,8}-19_{12,7}$	174905.610	12.8	246.4	[1]		
$21_{1,21}-20_{1,20}$	176638.245	20.9	94.8	176637.2	0.492	0.276
$23_{7,17}-22_{7,16}$	201117.777	20.9	169.8	201119.7	0.363[3]	0.578
$23_{7,16}-22_{7,15}$	201117.787	20.9	169.8	[1]		
$23_{12,12}-22_{12,11}$	201130.205	16.7	274.1	201129.7	0.227	0.326
$23_{12,11}-22_{12,10}$	201130.205	16.7	274.1	[1]		
$23_{3,21}-22_{3,20}$	201163.053	22.6	125.8	201162.2	0.570[3]	0.374
$23_{6,18}-22_{6,17}$	201199.149	21.4	155.5	201198.5	0.414	0.615
$23_{6,17}-22_{6,16}$	201199.658	21.4	155.5	[1]		
$23_{5,19}-22_{5,18}$	201355.689	21.9	143.4	201354.7	0.368	0.334
$24_{1,24}-23_{1,23}$	201501.280	23.9	122.6	201501.0	0.175	0.395
$23_{4,20}-22_{4,19}$	201562.025	22.3	133.6	201562.2	0.117	0.354
$23_{3,20}-22_{3,19}$	203831.883	22.6	126.4	203833.0	0.556[4]	0.377
$25_{1,25}-24_{1,24}$	209777.270	24.9	132.7	209780.8	0.189[3]	0.435
$24_{8,17}-23_{8,16}$	209830.348	21.3	196.3	209829.6	0.358	0.609
$24_{8,16}-23_{8,15}$	209830.348	21.3	196.3	[1]		
$24_{11,13}-23_{11,12}$	209839.700	19.0	258.9	209839.6	0.196	0.460
$24_{11,14}-23_{11,13}$	209839.700	19.0	258.9	[1]		
$24_{3,22}-23_{3,21}$	209845.011	23.6	135.9	209844.6	0.266	0.432
$24_{6,19}-23_{6,18}$	209970.955	22.5	165.5	209974.6	0.554[3]	0.681
$24_{6,18}-23_{6,17}$	209971.771	22.5	165.5	[1]		
$25_{0,25}-24_{0,24}$	209991.968	24.9	132.6	209989.6	0.422[13]	0.441
$24_{5,20}-23_{5,19}$	210149.174	23.0	153.5	210148.3	0.250	0.379
$24_{5,19}-23_{5,18}$	210173.298	23.0	153.5	210172.1	0.360	0.374
$24_{4,21}-23_{4,20}$	210362.161	23.3	143.7	210363.2	0.476[3]	0.398
$24_{4,20}-23_{4,19}$	210778.244	23.3	143.7	210778.3	0.149	0.398
$25_{2,24}-24_{2,23}$	215371.628	24.8	139.6	215372.0	0.691[14]	0.452
$26_{1,26}-25_{1,25}$	218048.481	25.9	143.1	218048.2	0.407	0.481
$25_{3,23}-24_{3,22}$	218509.862	24.6	146.4	218509.5	0.328	0.454
$25_{9,17}-24_{9,16}$	218560.501	21.8	225.5	218562.0	0.476	0.987
$25_{9,16}-24_{9,15}$	218560.501	21.8	225.5	[1]		
$25_{10,16}-24_{10,15}$	218562.285	21.0	246.4	[1]		
$25_{10,15}-24_{10,14}$	218562.285	21.0	246.4	[1]		
$25_{7,19}-24_{7,18}$	218635.678	23.0	190.3	218635.7	0.302	0.726

Table 9. continued.

Transitions J_{K_a,K_c}	predicted Frequency	S_{ij}	E_u/k (K)	Observed Frequency	Observed T_{mb} (K)	Model T_{mb} (K)
$25_{7,18}-24_{7,17}$	218635.709	23.0	190.3	[1]		
$25_{5,21}-24_{5,20}$	218946.860	24.0	164.0	218946.9	0.444	0.420
$25_{3,22}-24_{3,21}$	222137.470	24.6	147.3	222137.0	0.480	0.471
$25_{2,23}-24_{2,22}$	222942.719	24.8	143.1	222945.1	0.573[15]	0.486
$26_{2,25}-25_{2,24}$	223773.541	25.8	150.4	223774.4	0.576[3]	0.495
$26_{1,25}-25_{1,24}$	225837.819	25.8	149.8	225838.1	0.601[3]	0.508
$26_{3,24}-25_{3,23}$	227156.395	25.6	157.3	227156.3	0.354	0.498
$26_{11,15}-25_{11,14}$	227320.431	21.3	280.3	227320.6	0.760	0.550
$26_{11,16}-25_{11,15}$	227320.431	21.3	280.3	[1]		
$26_{12,14}-25_{12,13}$	227349.990	20.5	305.6	227346.8	0.664[9]	0.475
$26_{12,15}-25_{12,14}$	227349.990	20.5	305.6	[1]		
$26_{6,21}-25_{6,20}$	227523.781	24.6	187.0	227524.3	0.672	0.729
$26_{6,20}-25_{6,19}$	227525.754	24.6	187.0	[1]		
$26_{5,22}-25_{5,21}$	227748.628	25.0	174.9	227748.1	0.312	0.460
$26_{4,22}-25_{4,21}$	228659.559	25.4	165.2	228659.3	0.421	0.488
$26_{2,24}-25_{2,23}$	231662.988	25.8	154.2	231661.8	0.396	0.532
$27_{2,26}-26_{2,25}$	232158.356	26.8	161.5	232159.3	0.666	0.540
$28_{1,28}-27_{1,27}$	234578.648	27.9	165.2	234578.2	0.307	0.569
$27_{3,25}-26_{3,24}$	235783.549	26.7	168.6	235784.3	0.251	0.544
$27_{8,20}-26_{8,19}$	236085.740	24.6	229.1	236087.4	0.417	0.973
$27_{8,19}-26_{8,18}$	236085.741	24.6	229.1	[1]		
$27_{12,15}-26_{12,14}$	236088.731	21.7	316.9	[1]		
$27_{12,16}-26_{12,15}$	236088.731	21.7	316.9	[1]		
$27_{13,15}-26_{13,14}$	236129.081	20.7	344.3	236128.3	0.262	0.460
$27_{13,14}-26_{13,13}$	236129.081	20.7	344.3	[1]		
$27_{7,21}-26_{7,20}$	236160.863	25.2	212.6	236158.4	0.677[16]	0.882
$27_{7,20}-26_{7,19}$	236160.949	25.2	212.6	[1]		
$27_{14,14}-26_{14,13}$	236179.368	19.7	373.9	236178.4	0.317	0.397
$27_{14,13}-26_{14,12}$	236179.368	19.7	373.9	[1]		
$27_{6,22}-26_{6,21}$	236305.018	25.7	198.3	236307.0	0.951[3]	0.895
$27_{6,21}-26_{6,20}$	236308.004	25.7	198.3	[1]		
$27_{5,23}-26_{5,22}$	236554.279	26.1	186.3	236553.2	0.367	0.505
$27_{5,22}-26_{5,21}$	236622.668	26.1	186.3	236623.2	0.453	0.504
$28_{2,27}-27_{2,26}$	240526.926	27.8	173.1	240523.0	0.534[3]	0.584
$29_{0,29}-28_{0,28}$	242931.345	28.9	176.9	242930.3	0.598	0.614
$28_{10,19}-27_{10,18}$	244788.623	24.4	280.4	244787.2	0.976[17]	0.752
$28_{10,18}-27_{10,17}$	244788.623	24.4	280.4	[1]		
$28_{9,20}-27_{9,19}$	244798.948	25.1	259.5	244798.3	0.584	1.45
$28_{9,19}-27_{9,18}$	244798.948	25.1	259.5	[1]		
$28_{11,18}-27_{11,17}$	244799.670	23.7	303.4	[1]		
$28_{11,17}-27_{11,16}$	244799.670	23.7	303.4	[1]		
$28_{2,26}-27_{2,25}$	248935.100	27.8	177.7	248936.2	0.462	0.621
$30_{1,30}-29_{1,29}$	251095.276	29.9	188.9	251093.1	1.19[17]	0.657
$29_{3,27}-28_{3,26}$	252976.308	28.7	192.5	252976.1	1.03[3]	0.645
$29_{10,20}-28_{10,19}$	253530.604	25.6	292.5	253531.7	0.326	0.815
$29_{10,19}-28_{10,18}$	253530.604	25.6	292.5	[1]		
$29_{9,21}-28_{9,20}$	253545.867	26.2	271.7	253541.7	0.925[7]	0.904
$29_{9,20}-28_{9,19}$	253545.867	26.2	271.7	[1]		
$29_{6,24}-28_{6,23}$	253877.615	27.8	222.3	253876.1	0.340	0.573
$29_{6,23}-28_{6,22}$	253884.133	27.8	222.3	253885.1	0.910[3]	0.577
$29_{5,25}-28_{5,24}$	254175.975	28.1	210.3	254176.7	0.494	0.589
$29_{3,26}-28_{3,25}$	258689.348	28.7	194.3	258688.0	0.240	0.660
$31_{0,31}-30_{0,30}$	259409.260	30.9	201.4	259408.6	0.352	0.698
$30_{3,28}-29_{3,27}$	261540.638	29.7	205.0	261540.4	0.601	0.675
$30_{9,22}-29_{9,21}$	262293.189	27.3	284.2	262294.1	0.533	0.963
$30_{9,21}-29_{9,20}$	262293.189	27.3	284.2	[1]		
$30_{7,24}-29_{7,23}$	262463.576	28.4	249.1	262462.9	0.430	1.12
$30_{7,23}-29_{7,22}$	262463.913	28.4	249.1	[1]		
$30_{4,27}-29_{4,26}$	263084.409	29.5	213.1	263084.1	0.182	0.660
$30_{4,26}-29_{4,25}$	264787.920	29.5	213.5	264787.0	0.446	0.669
$30_{2,28}-29_{2,27}$	265968.647	29.8	202.8	265969.0	0.819[4]	0.709
$31_{1,30}-30_{1,29}$	266639.056	30.8	209.8	266640.9	0.388	0.720
$32_{1,32}-31_{1,31}$	267600.896	31.9	214.2	267601.3	0.922[7]	0.740
$32_{0,32}-31_{0,31}$	267648.851	31.9	214.2	267649.0	0.220	0.740
$30_{3,27}-29_{3,26}$	267765.153	29.7	207.2	267767.0	0.820[18]	0.707

Table 9. continued.

Transitions J_{K_a,K_c}	predicted Frequency	S_{ij}	E_u/k (K)	Observed Frequency	Observed T_{mb} (K)	Model T_{mb} (K)
$31_{10,22}$–$30_{10,21}$	271014.330	27.8	318.1	271014.0	0.376	1.69
$31_{10,21}$–$30_{10,20}$	271014.330	27.8	318.1	[1]		
$31_{11,21}$–$30_{11,20}$	271015.427	27.1	341.2	[1]		
$31_{11,20}$–$30_{11,19}$	271015.427	27.1	341.2	[1]		
$31_{12,19}$–$30_{12,18}$	271037.066	26.4	366.4	271040.2	0.459	1.17
$31_{12,20}$–$30_{12,19}$	271037.066	26.4	366.4	[1]		
$31_{9,23}$–$30_{9,22}$	271040.923	28.4	297.3	[1]		
$31_{9,22}$–$30_{9,21}$	271040.923	28.4	297.3	[1]		
$31_{13,19}$–$30_{13,18}$	271074.792	25.5	393.8	271080.1	0.658[5]	0.656
$31_{13,18}$–$30_{13,17}$	271074.792	25.5	393.8	[1]		
$31_{8,24}$–$30_{8,23}$	271107.321	28.9	278.6	271111.5	0.650[19]	1.11
$31_{8,23}$–$30_{8,22}$	271107.335	28.9	278.6	[1]		
$31_{16,15}$–$30_{16,14}$	271259.769	22.7	489.0	271259.0	0.292	0.425
$31_{16,16}$–$30_{16,15}$	271259.769	22.7	489.0	[1]		
$31_{6,25}$–$30_{6,24}$	271477.610	29.8	247.9	271477.7	0.622	0.643
$31_{5,27}$–$30_{5,26}$	271808.357	30.2	235.9	271807.9	0.506	0.577
$31_{4,28}$–$30_{4,27}$	271843.393	30.5	226.1	271842.8	0.712[8]	0.701
$32_{2,31}$–$31_{2,30}$	273858.228	31.8	223.2	273857.8	1.45[20]	0.751
$31_{4,27}$–$30_{4,26}$	273902.692	30.5	226.6	273901.8	0.481	0.713
$32_{2,29}$–$31_{2,28}$	274393.861	30.8	216.0	274392.8	0.560	0.751
$32_{1,31}$–$31_{1,30}$	274796.269	31.8	223.0	274795.8	0.958[3]	0.758
$31_{3,28}$–$30_{3,27}$	276802.146	30.7	220.5	276803.7	0.443	0.750
$32_{11,22}$–$31_{11,21}$	279753.114	28.2	354.6	279754.5	0.770	1.44
$32_{11,21}$–$31_{11,20}$	279753.114	28.2	354.6	[1]		
$32_{10,23}$–$31_{10,22}$	279756.064	28.9	331.6	279756.8	0.613	1.44
$32_{10,22}$–$31_{10,21}$	279756.064	28.9	331.6	[1]		
$32_{12,21}$–$31_{12,20}$	279772.360	27.5	379.9	279773.8	0.917[3]	0.805
$32_{12,20}$–$31_{12,19}$	279772.360	27.5	379.9	[1]		
$32_{9,24}$–$31_{9,23}$	279789.080	29.5	310.7	279788.8	0.765	1.08
$32_{9,23}$–$31_{9,22}$	279789.081	29.5	310.7	[1]		
$32_{13,20}$–$31_{13,19}$	279808.902	26.7	407.3	279809.8	0.439	0.701
$32_{13,19}$–$31_{13,18}$	279808.902	26.7	407.3	[1]		
$32_{14,18}$–$31_{14,17}$	279859.545	25.9	436.8	279858.8	0.558	0.617
$32_{14,19}$–$31_{14,18}$	279859.545	25.9	436.8	[1]		
$32_{8,25}$–$31_{8,24}$	279865.526	30.0	292.0	279865.8	0.923	1.14
$32_{8,24}$–$31_{8,23}$	279865.549	30.0	292.0	[1]		

[1] blended with the last one
[2] blended with c-C_3H_2
[3] blended with unidentified line
[4] blended with CH_3CH_2CN b type
[5] blended with CH_3OD
[6] blended with CCS
[7] blended with CH_3OCOH
[8] blended with CH_3COCH_3
[9] blended with $^{13}CH_3CH_2CN$
[10] blended with $SO^{18}O$
[11] blended with $HNC^{18}O$
[12] blended with SO_2 $\nu_2 = 1$
[13] blended with CH_3OCH_3
[14] blended with t-CH_3CH_2OH
[15] blended with $CH_3^{13}CH_2CN$
[16] blended with CH_2CHCN $\nu_{11} = 1$
[17] blended with CH_3CHO
[18] blended with $^{13}CH_3CN$
[19] blended with HCOOH
[20] blended with $S^{18}O$

Table 10. Emission lines of $CH_3^{13}CH_2CN$ (without high blend) present in the frequency range of the Orion KL survey. Column 1 indicates the transition, Col. 2 gives the calculated frequencies, Col. 3 gives the line strenght, Col. 4 the energy of the upper level, Col. 5 the observed (centroid) frequencies assuming that the radial velocities relative to LSR are 5 km s^{-1}, Col. 6 the observed temperature of main beam and Col. 7 gives the main beam temperature obtained with the model.

Transitions J_{K_a,K_c}	Predicted Frequency	S_{ij}	E_u/k (K)	Observed Frequency	Observed $T_{\rm mb}$ (K)	Model $T_{\rm mb}$ (K)
$10_{0,10}$–$9_{0,9}$	87799.440	9.98	23.3	87799.3	0.038	0.027
$10_{6,5}$–$9_{6,4}$	89122.309	6.40	62.5	89123.3	0.070	0.039
$10_{6,4}$–$9_{6,3}$	89122.309	6.40	62.5	[1]		
$10_{7,4}$–$9_{7,3}$	89123.598	5.10	76.6	[1]		
$10_{7,3}$–$9_{7,2}$	89123.597	5.10	76.6	[1]		
$10_{5,6}$–$9_{5,5}$	89129.924	7.50	50.6	89130.3	0.039	0.052
$10_{5,5}$–$9_{5,4}$	89129.935	7.50	50.6	[1]		
$10_{8,3}$–$9_{8,2}$	89130.352	3.60	92.8	[1]		
$10_{8,2}$–$9_{8,1}$	89130.352	3.60	92.8	[1]		
$10_{4,7}$–$9_{4,6}$	89154.636	8.40	40.9	89155.3	0.053	0.033
$10_{4,6}$–$9_{4,5}$	89155.808	8.40	40.9	[1]		
$10_{3,7}$–$9_{3,6}$	89259.164	9.10	33.3	89260.3	0.033	0.024
$10_{2,8}$–$9_{2,7}$	90079.324	9.60	28.0	90078.3	0.034	0.027
$10_{1,9}$–$9_{1,8}$	91139.116	9.89	25.2	91139.3	0.037	0.029
$11_{1,11}$–$10_{1,10}$	94867.175	10.9	28.5	94867.2	0.029	0.036
$11_{0,11}$–$10_{0,10}$	96329.800	11.0	27.9	96329.2	0.036	0.038
$11_{2,10}$–$10_{2,9}$	97672.054	10.6	32.5	97671.2	0.018	0.037
$11_{7,5}$–$10_{7,4}$	98039.620	6.55	81.3	98040.2	0.111	0.073
$11_{7,4}$–$10_{7,3}$	98039.620	6.55	81.3	[1]		
$11_{6,6}$–$10_{6,5}$	98040.577	7.73	67.2	[1]		
$11_{6,5}$–$10_{6,4}$	98040.577	7.73	67.2	[1]		
$11_{5,7}$–$10_{5,6}$	98052.972	8.73	55.3	98053.2	0.127[2]	0.058
$11_{5,6}$–$10_{5,5}$	98052.998	8.73	55.3	[1]		
$11_{9,2}$–$10_{9,1}$	98056.185	3.64	115.9	[1]		
$11_{9,3}$–$10_{9,2}$	98056.185	3.64	115.9	[1]		
$11_{4,8}$–$10_{4,7}$	98087.364	9.55	45.6	98088.2	0.041	0.037
$11_{4,7}$–$10_{4,6}$	98089.703	9.55	45.6	[1]		
$11_{3,9}$–$10_{3,8}$	98134.887	10.2	38.0	98135.2	0.052	0.035
$11_{1,10}$–$10_{1,9}$	100155.864	10.9	30.0	100155.2	0.030	0.041
$12_{1,12}$–$11_{1,11}$	103419.695	11.9	33.4	103420.1	0.60	0.49
$12_{0,12}$–$11_{0,11}$	104812.940	12.0	33.0	104813.1	0.078	0.051
$12_{2,11}$–$11_{2,10}$	106487.873	11.7	37.6	106488.1	0.023	0.050
$12_{7,6}$–$11_{7,5}$	106956.683	7.92	86.4	106956.2	0.086[3]	0.065
$12_{7,5}$–$11_{7,4}$	106956.683	7.92	86.4	[1]		
$12_{6,7}$–$11_{6,6}$	106960.564	9.00	72.4	106961.1	0.124	0.111
$12_{6,6}$–$11_{6,5}$	106960.564	9.00	72.4	[1]		
$12_{8,5}$–$11_{8,4}$	106961.311	6.67	102.7	[1]		
$12_{8,4}$–$11_{8,3}$	106961.311	6.67	102.7	[1]		
$12_{9,4}$–$11_{9,3}$	106971.702	5.25	121.0	106969.1	0.068[2]	0.034
$12_{9,3}$–$11_{9,2}$	106971.702	5.25	121.0	[1]		
$12_{5,8}$–$11_{5,7}$	106978.882	9.92	60.5	106979.0	0.077	0.080
$12_{5,7}$–$11_{5,6}$	106978.942	9.92	60.5	[1]		
$12_{4,9}$–$11_{4,8}$	107024.766	10.7	50.7	107024.0	0.115[4]	0.047
$12_{4,8}$–$11_{4,7}$	107029.140	10.7	50.7	107029.1	0.065	0.049
$12_{3,10}$–$11_{3,9}$	107076.493	11.2	43.1	107076.1	0.072	0.048
$12_{3,9}$–$11_{3,8}$	107235.540	11.2	43.2	107235.1	0.045	0.049
$12_{2,10}$–$11_{2,9}$	108510.623	11.7	38.0	108511.0	0.037	0.053
$13_{1,13}$–$12_{1,12}$	111957.777	12.9	38.8	111958.0	0.088	0.064
$13_{0,13}$–$12_{0,12}$	113255.691	13.0	38.4	113255.0	0.060	0.067
$15_{0,15}$–$14_{0,14}$	130052.739	14.9	50.5	130053.1	0.097	0.107
$15_{2,14}$–$14_{2,13}$	132834.311	14.7	55.5	132835.7	0.111	0.109
$15_{8,8}$–$14_{8,7}$	133712.843	10.7	120.6	133712.7	0.311[3]	0.179
$15_{8,7}$–$14_{8,6}$	133712.843	10.7	120.6	[1]		
$15_{7,9}$–$14_{7,8}$	133715.047	11.7	104.4	[1]		
$15_{7,8}$–$14_{7,7}$	133715.047	11.7	104.4	[1]		
$15_{6,10}$–$14_{6,9}$	133732.382	12.6	90.3	133732.7	0.263	0.177
$15_{6,9}$–$14_{6,8}$	133732.389	12.6	90.3	[1]		
$15_{10,5}$–$14_{10,4}$	133734.965	8.33	159.5	[1]		
$15_{10,6}$–$14_{10,5}$	133734.965	8.33	159.5	[1]		
$15_{3,13}$–$14_{3,12}$	133901.859	14.4	61.1	133901.7	0.166	0.106
$15_{1,14}$–$14_{1,13}$	135859.654	14.9	53.3	135859.6	0.132	0.118
$15_{2,13}$–$14_{2,12}$	136295.731	14.7	56.3	136297.1	0.139	0.117

Table 10. continued.

Transitions J_{K_a,K_c}	predicted Frequency	S_{ij}	E_u/k (K)	Observed Frequency	Observed $T_{\rm mb}$ (K)	Model $T_{\rm mb}$ (K)
$16_{1,16}$–$15_{1,15}$	137489.348	15.9	57.4	137489.5	0.335	0.128
$16_{0,16}$–$15_{0,15}$	138423.309	15.9	57.1	138424.5	0.215	0.131
$16_{2,15}$–$15_{2,14}$	141579.488	15.7	62.3	141579.6	0.206	0.134
$16_{7,10}$–$15_{7,9}$	142637.201	12.9	111.2	142636.6	0.191	0.332
$16_{7,9}$–$15_{7,8}$	142637.201	12.9	111.2	[1]		
$16_{9,8}$–$15_{9,7}$	142637.443	10.9	145.8	[1]		
$16_{9,7}$–$15_{9,6}$	142637.443	10.9	145.8	[1]		
$16_{11,5}$–$15_{11,4}$	142671.590	8.44	189.0	142672.6	0.118	0.092
$16_{11,6}$–$15_{11,5}$	142671.590	8.44	189.0	[1]		
$16_{5,12}$–$15_{5,11}$	142716.169	14.4	85.3	142719.6	0.372[5]	0.215
$16_{5,11}$–$15_{5,10}$	142717.034	14.4	85.3	[1]		
$16_{4,13}$–$15_{4,12}$	142824.845	15.0	75.6	142825.6	0.409[6]	0.125
$16_{3,14}$–$15_{3,13}$	142838.581	15.4	68.0	142837.6	0.147	0.131
$16_{4,12}$–$15_{4,11}$	142858.508	15.0	75.6	142857.6	0.315[7]	0.125
$16_{1,15}$–$15_{1,14}$	144671.483	15.9	60.5	144670.6	0.231	0.145
$17_{1,17}$–$16_{1,16}$	145974.513	16.9	64.4	145974.6	0.157	0.155
$17_{0,17}$–$16_{0,16}$	146784.555	16.9	64.2	146784.6	0.188	0.158
$17_{2,16}$–$16_{2,15}$	150304.830	16.8	69.5	150305.6	0.228	0.163
$17_{8,10}$–$16_{8,9}$	151551.211	13.2	134.7	151551.8	0.349[4]	0.221
$17_{8,9}$–$16_{8,8}$	151551.211	13.2	134.7	[1]		
$17_{9,9}$–$16_{9,8}$	151554.928	12.2	153.1	[1]		
$17_{9,8}$–$16_{9,7}$	151554.928	12.2	153.1	[1]		
$17_{7,11}$–$16_{7,10}$	151560.856	14.1	118.5	151561.9	0.287	0.249
$17_{7,10}$–$16_{7,9}$	151560.855	14.1	118.5	[1]		
$17_{5,13}$–$16_{5,12}$	151660.107	15.5	92.6	151660.5	0.406[4]	0.232
$17_{5,12}$–$16_{5,11}$	151661.614	15.5	92.6	[1]		
$17_{3,15}$–$16_{3,14}$	151769.770	16.5	75.3	151770.5	0.381[4]	0.162
$17_{4,13}$–$16_{4,12}$	151839.008	16.1	82.8	151838.5	0.173	0.152
$18_{0,18}$–$17_{0,17}$	155141.711	17.9	71.6	155144.3	0.240[8]	0.188
$18_{8,11}$–$17_{8,10}$	160471.756	14.4	142.4	160471.8	0.425	0.426
$18_{8,10}$–$17_{8,9}$	160471.756	14.4	142.4	[1]		
$18_{9,10}$–$17_{9,9}$	160472.884	13.5	160.8	[1]		
$18_{9,9}$–$17_{9,8}$	160471.884	13.5	160.8	[1]		
$18_{10,9}$–$17_{10,8}$	160484.712	12.4	181.4	160485.5	0.340	0.411
$18_{10,8}$–$17_{10,7}$	160484.712	12.4	181.4	[1]		
$18_{7,12}$–$17_{7,11}$	160486.105	15.3	126.2	[1]		
$18_{7,11}$–$17_{7,10}$	160486.105	15.3	126.2	[1]		
$18_{5,13}$–$17_{5,12}$	160610.877	16.6	100.3	160610.3	0.298	0.214
$18_{3,16}$–$17_{3,15}$	160693.493	17.5	83.0	160692.4	0.170	0.193
$18_{3,15}$–$17_{3,14}$	161813.575	17.5	83.2	161813.4	0.204	0.194
$19_{0,19}$–$18_{0,18}$	163498.529	18.9	79.5	163497.0	0.308[4]	0.220
$19_{2,18}$–$18_{2,17}$	167693.805	18.8	85.2	167694.2		
$19_{9,11}$–$18_{9,10}$	169391.337	14.7	169.0	169392.8	0.571[3]	0.439
$19_{9,10}$–$18_{9,9}$	169391.337	14.7	169.0	[1]		
$19_{8,12}$–$18_{8,11}$	169393.276	15.6	150.6	[1]		
$19_{8,11}$–$18_{8,10}$	169393.276	15.6	150.6	[1]		
$19_{10,10}$–$18_{10,9}$	169401.599	13.7	189.5	169401.6	0.269	0.247
$19_{10,9}$–$18_{10,8}$	169401.599	13.7	189.5	[1]		
$19_{7,13}$–$18_{7,12}$	169413.039	16.4	134.4	169414.2	0.391	0.347
$19_{7,12}$–$18_{7,11}$	169413.040	16.4	134.4	[1]		
$19_{12,8}$–$18_{12,7}$	169447.437	11.4	237.0	169449.1	0.320[4]	0.163
$19_{12,7}$–$18_{12,6}$	169447.437	11.4	237.0	[1]		
$19_{6,14}$–$18_{6,13}$	169461.556	17.1	120.3	169461.6	0.761[9]	0.375
$19_{6,13}$–$18_{6,12}$	169461.647	17.1	120.3	[1]		
$19_{5,15}$–$18_{5,14}$	169561.050	17.7	108.4	169561.6	0.368	0.281
$19_{5,14}$–$18_{5,13}$	169565.204	17.7	108.4	[1]		
$19_{3,17}$–$18_{3,16}$	169607.785	18.5	91.1	169608.2	0.296	0.271
$19_{4,15}$–$18_{4,14}$	169837.796	18.2	98.7	169838.2	0.222	0.216
$19_{3,16}$–$18_{3,15}$	171035.036	18.5	91.4	171036.6	0.448[8]	0.231
$22_{2,20}$–$21_{2,19}$	200514.457	21.8	114.4	200514.7	0.166	0.394
$24_{1,24}$–$23_{1,23}$	205107.677	23.9	124.8	205107.1	0.612	0.503
$23_{6,18}$–$22_{6,17}$	205237.944	21.4	157.1	205238.4	0.320	0.651
$23_{6,17}$–$22_{6,16}$	205238.716	21.4	157.1	[1]		
$24_{0,24}$–$23_{0,23}$	205331.591	23.9	124.7	205332.1	0.421	0.414
$23_{5,19}$–$22_{5,18}$	205419.492	21.9	145.3	205418.4	0.248	0.354

Table 10. continued.

Transitions J_{K_a,K_c}	predicted Frequency	S_{ij}	E_u/k (K)	Observed Frequency	Observed $T_{\rm mb}$ (K)	Model $T_{\rm mb}$ (K)
$23_{5,18}-22_{5,17}$	205442.696	21.9	145.3	205444.7	0.379[3]	0.354
$23_{4,20}-22_{4,19}$	205638.830	22.3	135.6	205638.4	0.340	0.357
$24_{2,23}-23_{2,22}$	210799.376	23.8	131.6	210799.5	0.323	0.428
$24_{1,23}-23_{1,22}$	213135.547	23.9	130.9	213134.6	0.359	0.429
$25_{1,25}-24_{1,24}$	213528.307	24.9	135.0	213529.5	0.511	0.458
$25_{0,25}-24_{0,24}$	213709.622	24.9	135.0	213708.3	0.647	0.459
$24_{3,22}-23_{3,21}$	213971.982	23.6	138.2	213970.8	0.471[3]	0.432
$24_{10,15}-23_{10,14}$	213988.615	19.8	236.6	213990.8	0.620[3]	0.667
$24_{10,14}-23_{10,13}$	213988.615	19.8	236.6	[1]		
$24_{9,16}-23_{9,15}$	213991.924	20.6	216.0	[1]		
$24_{9,15}-23_{9,14}$	213991.924	20.6	216.0	[1]		
$24_{11,13}-23_{11,12}$	214001.054	19.0	259.2	214001.4	0.377[5]	0.470
$24_{11,14}-23_{11,13}$	214001.054	19.0	259.2	[1]		
$24_{8,17}-23_{8,16}$	214017.318	21.3	197.7	214017.0	0.342	0.640
$24_{8,16}-23_{8,15}$	214017.318	21.3	197.7	[1]		
$24_{6,19}-23_{6,18}$	214190.553	22.5	167.4	214190.8	0.494	0.688
$24_{6,18}-23_{6,17}$	214191.790	22.5	167.4	[1]		
$24_{16,9}-23_{16,8}$	214206.257	13.3	404.5	214207.0	0.084	0.196
$24_{16,8}-23_{16,7}$	214206.257	13.3	404.5	[1]		
$24_{5,19}-23_{5,18}$	214430.179	23.0	155.6	214432.0	0.406[4]	0.399
$24_{4,21}-23_{4,20}$	214617.845	23.3	145.9	214620.7	0.469[8]	0.417
$24_{4,20}-23_{4,19}$	215156.584	23.3	146.0	215155.8	0.554[4]	0.491
$24_{3,21}-23_{3,20}$	217614.369	23.6	139.1	217614.5	0.648[10]	0.448
$26_{0,26}-25_{0,25}$	222090.574	25.9	145.6	222089.4	0.467	0.482
$25_{3,23}-24_{3,22}$	222791.617	24.6	148.9	222790.6	0.310	0.475
$25_{12,14}-24_{12,13}$	222939.994	19.2	294.7	222945.1	0.572[11]	0.474
$25_{12,13}-24_{12,12}$	222939.994	19.2	294.7	[1]		
$25_{8,18}-24_{8,17}$	222945.771	22.4	208.4	[1]		
$25_{8,17}-24_{8,16}$	222945.772	22.4	208.4	[1]		
$25_{13,13}-24_{13,12}$	222973.798	18.2	321.7	222970.7	0.618[3]	0.386
$25_{13,12}-24_{13,11}$	222973.798	18.2	321.7	[1]		
$25_{7,19}-24_{7,18}$	223015.182	23.0	192.1	223014.4	0.573	1.05
$25_{7,18}-24_{7,17}$	223015.233	23.0	192.1	[1]		
$25_{14,12}-24_{14,11}$	223016.365	17.2	350.7	[1]		
$25_{14,11}-24_{14,10}$	223016.365	17.2	350.7	[1]		
$25_{6,20}-24_{6,19}$	223146.857	23.6	178.1	223148.1	0.475	0.696
$25_{6,19}-24_{6,18}$	223148.797	23.6	178.1	[1]		
$25_{4,22}-24_{4,21}$	223594.386	24.4	156.6	223596.9	0.263	0.462
$25_{4,21}-24_{4,20}$	224297.114	24.4	156.7	[1]		
$25_{3,22}-24_{3,21}$	226974.990	24.6	150.0	226974.4	0.440	0.497
$26_{1,25}-25_{1,24}$	229803.538	25.8	152.6	229804.3	0.448[12]	0.530
$26_{3,24}-25_{3,23}$	231590.282	25.6	160.0	231593.2	0.610[13]	0.521
$26_{10,17}-25_{10,16}$	231824.731	22.2	258.4	231824.3	0.289[14]	0.659
$26_{10,16}-25_{10,15}$	231824.731	22.2	258.4	[1]		
$26_{11,15}-25_{11,14}$	231832.198	21.3	281.0	231833.0	0.173	0.645
$26_{11,16}-25_{11,15}$	231832.198	21.3	281.0	[1]		
$26_{9,18}-25_{9,17}$	231836.493	22.9	237.9	231836.8	0.226	0.760
$26_{9,17}-25_{9,16}$	231836.493	22.9	237.9	[1]		
$26_{8,19}-25_{8,18}$	231875.560	23.5	219.5	231871.8	0.349[5]	0.784
$26_{8,18}-25_{8,17}$	231875.562	23.5	219.5	[1]		
$26_{16,11}-25_{16,10}$	232039.545	16.2	426.3	232039.3	0.103	0.262
$26_{16,10}-25_{16,9}$	232039.545	16.2	426.3	[1]		
$26_{17,10}-25_{17,9}$	232104.322	14.9	461.7	232108.0	0.180	0.641
$26_{17,9}-25_{17,8}$	232104.322	14.9	461.7	[1]		
$26_{6,21}-25_{6,20}$	232106.987	24.6	189.2	[1]		
$26_{6,20}-25_{6,19}$	232109.974	24.6	189.2	[1]		
$26_{5,22}-25_{5,21}$	232363.924	25.0	177.4	232363.3	0.199	0.484
$26_{5,21}-25_{5,20}$	232432.713	25.0	177.4	232432.0	0.271	0.483
$26_{4,23}-25_{4,22}$	232566.761	25.4	167.8	232567.0	0.169	0.508
$26_{4,22}-25_{4,21}$	233470.034	25.4	168.0	233467.0	0.228[4]	0.512
$26_{3,23}-25_{3,22}$	236327.736	25.7	161.4	236328.2	0.248	0.546
$27_{2,26}-26_{2,25}$	236425.676	26.8	164.4	236425.7	0.374	0.564
$27_{1,26}-26_{1,25}$	238110.033	26.8	164.0	238111.3	0.350	0.576
$28_{0,28}-27_{0,27}$	238859.033	27.9	168.2	238860.3	0.474	0.576
$27_{3,25}-26_{3,24}$	240366.946	26.6	171.6	240368.0	0.571	0.569

Table 10. continued.

Transitions J_{K_a,K_c}	predicted Frequency	S_{ij}	E_u/k (K)	Observed Frequency	Observed T_{mb} (K)	Model T_{mb} (K)
$27_{12,15}$–$26_{12,14}$	240767.796	21.7	317.4	240764.2	0.790[3]	0.582
$27_{12,16}$–$26_{12,15}$	240767.796	21.7	317.4	[1]		
$27_{13,15}$–$26_{13,14}$	240800.499	20.7	344.4	240800.4	0.251	0.514
$27_{13,14}$–$26_{13,13}$	240800.499	20.7	344.4	[1]		
$27_{8,20}$–$26_{8,19}$	240806.735	24.6	231.0	240806.6	0.504	0.869
$27_{8,19}$–$26_{8,18}$	240806.738	24.6	231.0	[1]		
$27_{7,21}$–$26_{7,20}$	240900.244	25.2	214.8	240900.4	0.826	0.938
$27_{7,20}$–$26_{7,19}$	240900.383	25.2	214.8	[1]		
$27_{6,22}$–$26_{6,21}$	241071.065	25.7	200.8	241074.4	0.411	0.540
$27_{6,21}$–$26_{6,20}$	241075.583	25.7	200.8	[1]		
$27_{5,23}$–$26_{5,22}$	241354.267	26.1	189.0	241354.4	0.740[4]	0.530
$27_{5,22}$–$26_{5,21}$	241450.030	26.1	189.0	241449.4	0.916[3]	0.530
$27_{2,25}$–$26_{2,24}$	245004.430	26.8	169.0	245005.2	0.862	0.604
$27_{3,24}$–$26_{3,23}$	245662.389	26.7	173.2	245661.2	0.374	0.595
$29_{0,29}$–$28_{0,28}$	247245.507	28.9	180.0	247246.9	0.627	0.639
$28_{13,15}$–$27_{13,14}$	249712.876	22.0	356.3	249710.1	0.757[8]	0.539
$28_{13,16}$–$27_{13,15}$	249712.876	22.0	356.3	[1]		
$28_{7,22}$–$27_{7,21}$	249846.517	26.3	226.8	249846.2	0.782	1.01
$28_{7,21}$–$27_{7,20}$	249846.740	26.3	226.8	[1]		
$28_{17,12}$–$27_{17,11}$	249936.679	17.7	485.3	249937.2	0.110	0.280
$28_{17,11}$–$27_{17,10}$	249936.679	17.7	485.3	[1]		
$29_{2,28}$–$28_{2,27}$	253425.145	28.8	188.4	253424.2	0.516	0.655
$28_{2,26}$–$27_{2,25}$	253716.782	27.8	181.2	253716.1	1.19[8]	0.651
$29_{11,19}$–$28_{11,18}$	258577.731	24.8	317.0	258576.1	0.342	[15]
$29_{11,18}$–$28_{11,17}$	258577.731	24.8	317.0	[1]		
$29_{10,20}$–$28_{10,19}$	258580.432	25.6	294.3	258579.0	0.342	1.23
$29_{10,19}$–$28_{10,18}$	258580.432	25.6	294.3	[1]		
$29_{12,18}$–$28_{12,17}$	258593.828	24.0	341.8	258594.1	0.136	0.686
$29_{12,17}$–$28_{12,16}$	258593.828	24.0	341.8	[1]		
$29_{9,21}$–$28_{9,20}$	258608.583	26.2	273.8	258609.0	0.271	0.942
$29_{9,20}$–$28_{9,19}$	258608.583	26.2	273.8	[1]		
$29_{7,23}$–$28_{7,22}$	258795.413	27.3	239.2	258797.0	0.798	1.09
$29_{7,22}$–$28_{7,21}$	258795.766	27.3	239.2	[1]		
$29_{2,27}$–$28_{2,26}$	262362.311	28.8	193.7	262360.3	0.596	0.694
$31_{1,31}$–$30_{1,30}$	263973.471	30.9	205.0	263973.0	0.549	0.727
$31_{0,31}$–$30_{0,30}$	264020.728	30.9	205.0	264020.0	0.677	0.726
$29_{3,26}$–$28_{3,25}$	264241.006	28.7	198.1	264240.3	0.781[4]	0.693
$30_{3,28}$–$29_{3,27}$	266557.689	29.7	208.7	266556.6	0.284	0.703
$30_{8,23}$–$29_{8,22}$	267609.104	27.9	268.3	267609.9	1.10[5]	1.08
$30_{8,22}$–$29_{8,21}$	267609.119	27.9	268.3	[1]		
$30_{7,24}$–$29_{7,23}$	267747.028	28.4	252.1	267748.0	0.605	1.16
$30_{7,23}$–$29_{7,22}$	267747.577	28.4	252.1	[1]		
$30_{5,26}$–$29_{5,25}$	268345.778	29.2	226.3	268344.1	1.03[4]	0.659
$30_{4,27}$–$29_{4,26}$	268377.483	29.5	216.7	268376.5	0.372	0.690
$31_{1,30}$–$30_{1,29}$	271301.801	30.8	213.7	271302.7	0.260	0.747
$32_{1,32}$–$31_{1,31}$	272371.348	31.9	218.1	272369.0	0.651[16]	0.769
$31_{13,19}$–$30_{13,18}$	276445.791	25.5	394.9	276445.2	0.271	0.689
$31_{13,18}$–$30_{13,17}$	276445.791	25.5	394.9	[1]		
$31_{9,23}$–$30_{9,22}$	276460.408	28.4	299.9	276462.0	0.258	1.07
$31_{9,22}$–$30_{9,21}$	276460.409	28.4	299.9	[1]		
$31_{6,26}$–$30_{6,25}$	276968.682	29.8	251.4	276969.8	0.873	0.665
$31_{6,25}$–$30_{6,24}$	276968.949	29.8	251.4	[1]		
$31_{4,28}$–$30_{4,27}$	277300.828	30.5	230.0	277301.4	0.330	0.731
$31_{5,27}$–$30_{5,26}$	277347.421	30.2	239.7	277343.9	0.703[4]	0.702
$32_{2,31}$–$31_{2,30}$	278820.152	31.8	227.3	278820.7	1.21[17]	0.781
$32_{1,31}$–$31_{1,30}$	279609.687	31.8	227.1	279608.8	0.902	0.786

[1] blended with the last one
[2] blended with CH_3OCH_3
[3] blended with $^{13}CH_3CH_2CN$
[4] blended with unidentified line
[5] blended with $CH_3C^{15}N$
[6] blended with CH_2CHCN ν_{11} = 1
[7] blended with $^{13}CH_3CN$
[8] blended with CH_3OCOH

[9] blended with CH_3CH_2CN b type
[10] blended with c-C_2H_4O
[11] blended with $CH_3CH_2^{13}CN$
[12] blended with CH_3COCH_3
[13] blended with CH_3CHO
[14] blended with $CH_3^{18}OH$
[15] line blended with the transition: $J = 29-28$, $k = 10$
[16] blended with $H^{13}CCCN$ $\nu_7 = 1$
[17] blended with CH_3CH_2CN (high energy transition)

Table 11. Emission lines of $^{13}CH_3CH_2CN$ (without high blend) present in the frequency range of the Orion KL survey. Column 1 indicates the transition, Col. 2 gives the calculated frequencies, Col. 3 gives the line strenght, Col. 4 the energy of the upper level, Col. 5 the observed centroid frequencies assuming that the radial velocities relative to LSR are 5 km s^{-1}, Col. 6 the observed temperature of main beam and Col. 7 gives the main beam temperature obtained with the model.

Transitions J_{K_a,K_c}	Predicted Frequency	S_{ij}	E_u/k (K)	Observed Frequency	Observed $T_{\rm mb}$ (K)	Model $T_{\rm mb}$ (K)
$9_{2,7}-8_{2,6}$	80848.938	8.55	23.8	80849.4	0.020	0.018
$10_{1,10}-9_{1,9}$	86398.476	9.90	24.0	86398.2	0.048	0.026
$10_{2,9}-9_{2,8}$	88855.082	9.60	27.9	88855.3	0.022	0.026
$10_{6,5}-9_{6,4}$	89116.024	6.40	63.5	89116.3	0.036	0.034
$10_{6,4}-9_{6,3}$	89116.024	6.40	63.5	[1]		
$10_{7,4}-9_{7,3}$	89118.946	5.10	78.0	[1]		
$10_{7,3}-9_{7,2}$	89118.946	5.10	78.0	[1]		
$10_{5,6}-9_{5,5}$	89121.500	7.50	51.3	89121.3	0.070	0.042
$10_{5,5}-9_{5,4}$	89121.507	7.50	51.3	[1]		
$10_{4,7}-9_{4,6}$	89142.905	8.40	41.3	89142.3	0.051	0.030
$10_{4,6}-9_{4,5}$	89143.858	8.40	41.3	[1]		
$10_{3,7}-9_{3,6}$	89235.657	9.10	33.5	89236.3	0.028	0.025
$10_{1,9}-9_{1,8}$	91089.001	9.89	25.2	91089.3	0.046	0.30
$11_{1,11}-10_{1,10}$	94979.834	10.9	28.5	94981.3	0.055	0.036
$11_{0,11}-10_{0,10}$	96452.609	11.0	28.0	96452.3	0.048	0.038
$11_{7,5}-10_{7,4}$	98033.905	6.55	82.7	98033.2	0.063	0.071
$11_{7,4}-10_{7,3}$	98033.905	6.55	82.7	[1]		
$11_{5,7}-10_{5,6}$	98042.553	8.73	56.0	98043.2	0.146[2]	0.072
$11_{5,6}-10_{5,5}$	98042.573	8.73	56.0	[1]		
$11_{4,8}-10_{4,7}$	98072.727	9.55	46.0	98074.2	0.053	0.040
$11_{4,7}-10_{4,6}$	98074.629	9.55	46.0	[1]		
$11_{3,9}-10_{3,8}$	98117.427	10.2	38.2	98118.2	0.066	0.035
$11_{3,8}-10_{3,7}$	98206.224	10.2	38.3	98206.2	0.113[3]	0.035
$11_{2,9}-10_{2,8}$	99172.533	10.6	32.9	99171.2	0.045	0.040
$11_{1,10}-10_{1,9}$	100109.745	10.9	30.0	100110.2	0.089	0.042
$12_{2,11}-11_{2,10}$	106514.269	11.7	37.7	106514.1	0.050	0.051
$12_{7,6}-11_{7,5}$	106949.734	7.92	87.8	106951.1	0.097	0.094
$12_{7,5}-11_{7,4}$	106949.734	7.92	87.8	[1]		
$12_{6,7}-11_{6,6}$	106951.185	9.00	73.4	[1]		
$12_{6,6}-11_{6,5}$	106951.186	9.00	73.4	[1]		
$12_{8,5}-11_{8,4}$	106956.373	6.67	104.5	106956.1	0.086[3]	0.051
$12_{8,4}-11_{8,3}$	106956.373	6.67	104.5	[1]		
$12_{5,8}-11_{5,7}$	106966.140	9.92	61.2	106966.1	0.085	0.084
$12_{5,7}-11_{5,6}$	106966.186	9.92	61.2	[1]		
$12_{9,4}-11_{9,3}$	106968.595	5.25	123.3	106969.1	0.068	0.048
$12_{9,3}-11_{9,2}$	106968.595	5.25	123.3	[1]		
$12_{4,9}-11_{4,8}$	107006.773	10.7	51.2	107006.1	0.136[3]	0.052
$12_{2,10}-11_{2,9}$	108383.128	11.7	38.1	108383.0	0.068	0.054
$12_{1,11}-11_{1,10}$	109101.861	11.9	35.2	109102.0	0.065	0.057
$13_{1,13}-12_{1,12}$	112101.559	12.9	38.9	112102.0	0.082	0.065
$13_{0,13}-12_{0,12}$	113432.875	13.0	38.4	113430.0	0.156[3]	0.068
$15_{7,9}-14_{7,8}$	133703.216	11.7	105.8	133705.7	0.147	0.245
$15_{7,8}-14_{7,7}$	133703.216	11.7	105.8	[1]		
$15_{8,8}-14_{8,7}$	133704.214	10.7	122.4	[1]		
$15_{8,7}-14_{8,6}$	133704.214	10.7	122.4	[1]		
$15_{9,7}-14_{9,6}$	133714.526	9.60	141.3	133714.7	0.310	0.200
$15_{9,6}-14_{9,5}$	133714.526	9.60	141.3	[1]		
$15_{6,10}-14_{6,9}$	133716.429	12.6	91.3	[1]		
$15_{6,9}-14_{6,8}$	133716.434	12.6	91.3	[1]		
$15_{5,11}-14_{5,10}$	133754.340	13.3	79.1	133754.7	0.290	0.244
$15_{5,10}-14_{5,9}$	133754.706	13.3	79.1	[1]		
$15_{4,12}-14_{4,11}$	133836.322	13.9	69.1	133836.7	0.152	0.101
$15_{3,13}-14_{3,12}$	133876.070	14.4	61.4	133875.7	0.152	0.107
$15_{3,12}-14_{3,11}$	134288.098	14.4	61.4	134287.1	0.170	0.107
$15_{1,14}-14_{1,13}$	135865.172	14.9	53.5	135864.7	0.114	0.119
$15_{2,13}-14_{2,12}$	136120.886	14.7	56.3	136120.8	0.149	0.118
$16_{1,16}-15_{1,15}$	137684.426	15.9	57.5	137685.7	0.229[3]	0.130
$16_{0,16}-15_{0,15}$	138673.130	15.9	57.2	138673.7	0.161	0.132
$16_{6,11}-15_{6,10}$	142642.043	13.8	98.2	142641.6	0.183	0.216
$16_{6,10}-15_{6,9}$	142642.052	13.8	98.2	[1]		
$16_{11,5}-15_{11,4}$	142670.080	8.44	192.4	142669.6	0.118	0.091
$16_{11,6}-15_{11,5}$	142670.080	8.44	192.4	[1]		

Table 11. continued.

Transitions J_{K_a,K_c}	predicted Frequency	S_{ij}	E_u/k (K)	Observed Frequency	Observed T_{mb} (K)	Model T_{mb} (K)
$16_{5,12}-15_{5,11}$	142690.279	14.4	86.0	142690.6	0.355[4]	0.223
$16_{5,11}-15_{5,10}$	142690.942	14.4	86.0	[1]		
$16_{4,13}-15_{4,12}$	142788.956	15.0	76.0	142788.6	0.247[3]	0.126
$16_{1,15}-15_{1,14}$	144700.918	15.9	60.5	144701.6	0.188	0.148
$16_{2,14}-15_{2,13}$	145371.524	15.8	63.3	145370.7	0.131	0.146
$17_{1,17}-16_{1,16}$	146187.443	16.9	64.5	146185.7	0.175	0.157
$17_{8,10}-16_{8,9}$	151539.231	13.2	136.5	151540.1	0.200	0.222
$17_{8,9}-16_{8,8}$	151539.231	13.2	136.5	[1]		
$17_{7,11}-16_{7,10}$	151544.629	14.1	119.9	151545.6	0.255	0.319
$17_{7,10}-16_{7,9}$	151544.629	14.1	119.9	[1]		
$17_{9,9}-16_{9,8}$	151546.481	12.2	155.4	[1]		
$17_{9,8}-16_{9,7}$	151546.481	12.2	155.4	[1]		
$17_{12,6}-16_{12,5}$	151614.701	8.53	225.2	151615.5	0.251[5]	0.096
$17_{12,5}-16_{12,4}$	151614.701	8.53	225.2	[1]		
$17_{5,13}-16_{5,12}$	151629.833	15.5	93.3	151629.5	0.587[3]	0.253
$17_{5,12}-16_{5,11}$	151630.990	15.5	93.3	[1]		
$17_{3,15}-16_{3,14}$	151744.014	16.5	75.5	151744.5	0.59	0.208
$17_{4,14}-16_{4,13}$	151746.231	16.1	83.3	[1]		
$17_{2,15}-16_{2,14}$	154609.632	16.8	70.7	154609.4	0.275	0.177
$18_{1,18}-17_{1,17}$	154679.365	17.9	71.9	154679.4	0.208	0.188
$18_{8,11}-17_{8,10}$	160457.796	14.4	144.2	160458.0	0.383	0.268
$18_{8,10}-17_{8,9}$	160457.796	14.4	144.2	[1]		
$18_{9,10}-17_{9,9}$	160462.906	13.5	163.1	160463.0	0.269	0.261
$18_{9,9}-17_{9,8}$	160462.906	13.5	163.1	[1]		
$18_{7,12}-17_{7,11}$	160467.290	15.3	127.6	160467.9	0.349	0.308
$18_{7,11}-17_{7,10}$	160467.290	15.3	127.6	[1]		
$18_{6,13}-17_{6,12}$	160499.863	16.0	113.2	160500.5	0.409	0.401
$18_{6,12}-17_{6,11}$	160499.899	16.0	113.2	[1]		
$18_{11,8}-17_{11,7}$	160501.426	11.3	207.4	[1]		
$18_{11,7}-17_{11,6}$	160501.426	11.3	207.4	[1]		
$18_{3,16}-17_{3,15}$	160669.490	17.5	83.2	160671.4	0.282[7]	0.193
$18_{4,15}-17_{4,14}$	160707.921	17.1	91.0	160708.4	0.237	0.185
$18_{4,14}-17_{4,13}$	160770.345	17.1	91.0	160769.3	0.311	0.184
$18_{1,17}-17_{1,16}$	162220.345	17.9	75.6	162220.5	0.424[6]	0.209
$19_{0,19}-18_{0,18}$	163802.317	18.9	79.6	163802.3	0.281	0.222
$19_{2,18}-18_{2,17}$	167806.016	18.8	85.3	167805.3	0.368[3]	0.230
$19_{8,12}-18_{8,11}$	169377.118	15.6	152.4	169379.1	0.375	0.370
$19_{8,11}-18_{8,10}$	169377.118	15.6	152.4	[1]		
$19_{9,11}-18_{9,10}$	169379.651	14.7	171.2	[1]		
$19_{9,10}-18_{9,9}$	169379.651	14.7	171.2	[1]		
$19_{7,13}-18_{7,12}$	169391.355	16.4	135.7	169392.8	0.571[2]	0.398
$19_{7,12}-18_{7,11}$	169391.356	16.4	135.7	[1]		
$19_{10,10}-18_{10,9}$	169393.825	13.7	192.3	[1]		
$19_{10,9}-18_{10,8}$	169393.825	13.7	192.3	[1]		
$19_{5,15}-18_{5,14}$	169520.545	17.7	109.1	169520.3	0.359	0.237
$19_{5,14}-18_{5,13}$	169523.733	17.7	109.1	[1]		
$19_{3,17}-18_{3,16}$	169586.931	18.5	91.4	169587.2	0.418	0.227
$19_{4,16}-18_{4,17}$	169673.658	18.2	99.1	169673.3	0.308	0.229
$19_{3,16}-18_{3,15}$	170836.180	18.5	91.6	170835.2	0.244	0.320
$20_{1,20}-19_{1,19}$	171633.311	19.9	88.0	171632.2	0.186	0.257
$19_{2,17}-18_{2,16}$	173018.908	18.8	86.9	173017.8	0.356	0.247
$22_{3,19}-21_{3,18}$	198612.272	21.6	118.9	198613.4	0.164	0.356
$22_{2,20}-21_{2,19}$	200382.276	21.8	114.4	200382.2	0.149	0.374
$23_{2,22}-22_{2,21}$	202408.825	22.8	121.7	202408.0	0.507[8]	0.391
$23_{6,18}-22_{6,17}$	205189.043	21.4	158.1	205190.9	0.416	0.832
$23_{6,17}-22_{6,16}$	205189.602	21.4	158.1	[1]		
$23_{14,9}-22_{14,8}$	205190.642	14.5	335.3	[1]		
$23_{14,10}-22_{14,9}$	205190.642	14.5	335.3	[1]		
$23_{5,18}-22_{5,17}$	205370.323	21.9	145.9	205370.8	0.337	0.361
$24_{1,24}-23_{1,23}$	205445.595	23.9	125.0	205444.7	0.379	0.420
$23_{4,20}-22_{4,19}$	205564.319	22.3	136.0	205563.4	0.215	0.377
$23_{4,19}-22_{4,18}$	205898.051	22.3	136.1	205899.7	0.153	0.377
$23_{3,20}-22_{3,19}$	207927.839	22.6	128.8	207927.1	0.860[3]	0.402
$24_{1,23}-23_{1,22}$	213478.336	23.9	131.0	213474.6	0.698[3]	0.450
$25_{1,25}-24_{1,24}$	213883.341	24.9	135.2	213883.3	0.290	0.464

Table 11. continued.

Transitions J_{K_a,K_c}	predicted Frequency	S_{ij}	E_u/k (K)	Observed Frequency	Observed T_{mb} (K)	Model T_{mb} (K)
$24_{9,16}$–$23_{9,15}$	213968.681	20.6	218.3	213970.8	0.471[2]	0.702
$24_{9,15}$–$23_{9,14}$	213968.681	20.6	218.3	[1]		
$24_{10,15}$–$23_{10,14}$	213971.696	19.8	239.4	[1]		
$24_{10,14}$–$23_{10,13}$	213971.696	19.8	239.4	[1]		
$24_{8,17}$–$23_{8,16}$	213986.445	21.3	199.4	213990.8	0.620	0.685
$24_{8,16}$–$23_{8,15}$	213986.446	21.3	199.4	[1]		
$24_{11,14}$–$23_{11,13}$	213989.714	19.0	262.6	[1]		
$24_{11,13}$–$23_{11,12}$	213989.714	19.0	262.6	[1]		
$24_{3,22}$–$23_{3,21}$	213992.351	23.6	138.5	[1]		
$24_{7,18}$–$23_{7,17}$	214035.383	22.0	182.8	214038.3	0.486	0.693
$24_{7,17}$–$23_{7,16}$	214035.402	22.0	182.8	[1]		
$25_{0,25}$–$24_{0,24}$	214093.827	24.9	135.2	214092.0	0.551	0.458
$24_{6,19}$–$23_{6,18}$	214135.573	22.5	168.4	214137.0	0.526	0.716
$24_{6,18}$–$23_{6,17}$	214136.468	22.5	168.4	[1]		
$24_{17,8}$–$23_{17,7}$	214286.127	12.0	447.9	214285.7	0.123	0.150
$24_{17,7}$–$23_{17,6}$	214286.127	12.0	447.9	[1]		
$24_{5,20}$–$23_{5,19}$	214321.447	23.0	156.2	214320.8	0.335	0.398
$24_{4,21}$–$23_{4,20}$	214539.290	23.3	146.3	214539.5	0.193	0.420
$24_{4,20}$–$23_{4,19}$	214982.257	23.3	146.4	214980.8	0.454	0.422
$24_{3,21}$–$23_{3,20}$	217261.059	23.6	139.3	217260.7	0.635[9]	0.450
$25_{2,24}$–$24_{2,23}$	219592.890	24.8	142.3	219591.3	0.366	0.480
$25_{1,24}$–$24_{1,23}$	221861.413	24.9	141.6	221860.7	0.316	0.494
$26_{0,26}$–$25_{0,25}$	222487.587	25.9	145.9	222488.2	0.600[3]	0.512
$25_{10,16}$–$24_{10,15}$	222887.262	21.0	250.1	222888.1	0.572	1.21
$25_{10,15}$–$24_{10,14}$	222887.262	21.0	250.1	[1]		
$25_{9,17}$–$24_{9,16}$	222887.646	21.8	229.0	[1]		
$25_{9,16}$–$24_{9,15}$	222887.646	21.8	229.0	[1]		
$25_{7,19}$–$24_{7,18}$	222969.459	23.0	193.5	222970.7	0.618	1.01
$25_{7,18}$–$24_{7,17}$	222969.493	23.0	193.5	[1]		
$25_{13,13}$–$24_{13,12}$	222971.384	18.2	326.4	[1]		
$25_{13,12}$–$24_{13,11}$	222971.384	18.2	326.4	[1]		
$25_{6,20}$–$24_{6,19}$	223085.294	23.6	179.1	223085.7	0.522	0.762
$25_{6,19}$–$24_{6,18}$	223086.701	23.6	179.1	[1]		
$25_{5,21}$–$24_{5,20}$	223294.778	24.0	166.9	223293.2	0.709[3]	0.431
$25_{5,20}$–$24_{5,19}$	223332.274	24.0	167.0	223330.7	0.615[10]	0.443
$25_{4,22}$–$24_{4,21}$	223512.772	24.4	157.0	223511.9	0.663[11]	0.466
$25_{3,22}$–$24_{3,21}$	226603.238	24.6	150.1	226603.1	0.323	0.500
$25_{2,23}$–$24_{2,22}$	227346.679	24.8	145.9	227346.8	0.664[7]	0.516
$26_{1,25}$–$25_{1,24}$	230216.201	25.8	152.7	230216.8	0.336	0.539
$26_{3,24}$–$25_{3,23}$	231640.328	25.6	160.3	231640.5	0.319	0.528
$26_{10,17}$–$25_{10,16}$	231802.817	22.2	261.2	231806.7	0.210	0.776
$26_{10,16}$–$25_{10,15}$	231802.817	22.2	261.2	[1]		
$26_{9,18}$–$25_{9,17}$	231807.029	22.9	240.1	[1]		
$26_{9,17}$–$25_{9,16}$	231807.029	22.9	240.1	[1]		
$26_{8,19}$–$25_{8,18}$	231836.826	23.5	221.3	231836.8	0.232	0.793
$26_{8,18}$–$25_{8,17}$	231836.826	23.5	221.3	[1]		
$26_{5,21}$–$25_{5,20}$	232325.372	25.0	178.1	232325.7	0.201	0.487
$26_{4,23}$–$25_{4,22}$	232483.305	25.4	168.2	232484.5	0.230	0.513
$27_{2,26}$–$26_{2,25}$	236704.158	26.8	164.7	236702.0	0.586[3]	0.571
$27_{1,26}$–$26_{1,25}$	238550.531	26.8	164.1	238548.2	0.688[3]	0.584
$28_{1,28}$–$27_{1,27}$	239169.936	27.9	168.5	239169.9	0.473	0.603
$28_{0,28}$–$27_{0,27}$	239282.049	27.9	168.4	239282.0	0.768[3]	0.602
$27_{8,20}$–$26_{8,19}$	240763.594	24.6	232.8	240764.2	0.818	0.876
$27_{8,19}$–$26_{8,18}$	240763.596	24.6	232.8	[1]		
$27_{7,21}$–$26_{7,20}$	240843.497	25.2	216.2	240843.0	0.696	1.33
$27_{7,20}$–$26_{7,19}$	240843.592	25.2	216.2	[1]		
$27_{14,13}$–$26_{14,12}$	240844.057	19.7	378.9	[1]		
$27_{14,14}$–$26_{14,13}$	240844.057	19.7	378.9	[1]		
$27_{5,23}$–$26_{5,22}$	241253.894	26.1	189.7	241254.4	0.553[8]	0.531
$27_{4,24}$–$26_{4,23}$	241449.311	26.4	179.8	241449.4	0.916[2]	0.560
$28_{2,27}$–$27_{2,26}$	245234.539	27.8	176.4	245235.6	0.728	0.618
$27_{3,24}$–$26_{3,23}$	245276.518	26.7	173.2	245276.9	0.663	0.600
$29_{1,29}$–$28_{1,28}$	247591.507	28.9	180.3	247591.1	0.650	0.648
$28_{10,19}$–$27_{10,18}$	249633.880	24.4	284.7	249634.1	1.07	0.791
$28_{10,18}$–$27_{10,17}$	249633.880	24.4	284.7	[1]		

Table 11. continued.

Transitions J_{K_a,K_c}	predicted Frequency	S_{ij}	E_u/k (K)	Observed Frequency	Observed $T_{\rm mb}$ (K)	Model $T_{\rm mb}$ (K)
$28_{8,21}-27_{8,20}$	249691.465	25.7	244.8	249692.1	0.875	0.939
$28_{8,20}-27_{8,19}$	249691.468	25.7	244.8	[1]		
$28_{13,16}-27_{13,15}$	249706.003	22.0	361.1	249707.2	0.704	0.543
$28_{13,15}-27_{13,14}$	249706.003	22.0	361.1	[1]		
$28_{6,23}-27_{6,22}$	249954.742	26.7	213.8	249955.1	0.461	0.847
$28_{6,22}-27_{6,21}$	249959.619	26.7	213.8	[1]		
$28_{2,26}-27_{2,25}$	253822.050	27.8	181.2	253822.1	0.564	0.657
$30_{1,30}-29_{1,29}$	256010.058	29.9	192.6	256010.5	0.398	0.692
$29_{9,21}-28_{9,20}$	258567.815	26.2	276.1	258568.0	0.355	0.941
$29_{9,20}-28_{9,19}$	258567.815	26.2	276.1	[1]		
$29_{12,18}-28_{12,17}$	258578.344	24.0	345.9	258579.0	0.342[2]	0.685
$29_{12,17}-28_{12,16}$	258578.344	24.0	345.9	[1]		
$29_{8,22}-28_{8,21}$	258620.477	26.8	257.2	258620.0	0.302	1.06
$29_{8,21}-28_{8,20}$	258620.483	26.8	257.2	[1]		
$29_{7,23}-28_{7,22}$	258725.899	27.3	240.6	258724.1	0.316	1.41
$29_{7,22}-28_{7,21}$	258726.141	27.3	240.6	[1]		
$29_{4,26}-28_{4,25}$	259360.994	28.4	204.3	259359.2	0.323	0.714
$29_{5,24}-28_{5,23}$	259365.473	28.1	214.1	259362.9	0.239	0.694
$29_{4,25}-28_{4,24}$	260836.777	28.4	204.6	260837.0	0.403	0.658
$31_{0,31}-30_{0,30}$	264483.855	30.9	205.3	264485.4	0.445	0.736
$30_{3,28}-29_{3,27}$	266688.918	29.7	209.0	266686.0	0.477	0.711
$30_{10,21}-29_{10,20}$	267464.848	26.7	310.0	267466.5	0.355	1.51
$30_{10,20}-29_{10,19}$	267464.848	26.7	310.0	[1]		
$30_{11,20}-29_{11,19}$	267466.842	26.0	333.2	[1]		
$30_{11,19}-29_{11,18}$	267466.842	26.0	333.2	[1]		
$30_{7,24}-29_{7,23}$	267670.433	28.4	253.5	267669.9	0.158	1.17
$30_{7,23}-29_{7,22}$	267670.808	28.4	253.5	[1]		
$30_{5,26}-29_{5,25}$	268218.881	29.2	227.0	268216.6	0.625	0.664
$30_{4,26}-29_{4,25}$	270107.598	16.3	217.5	270107.8	1.25[8]	0.704
$31_{2,30}-30_{2,29}$	270736.607	30.8	214.2	270735.9	1.22[3]	0.750
$30_{2,28}-29_{2,27}$	271166.987	29.8	206.8	271165.3	0.463	0.746
$31_{1,30}-30_{1,29}$	271812.173	30.8	213.9	271810.9	0.506	0.756
$32_{1,32}-31_{1,31}$	272839.201	31.8	218.4	272838.8	1.16[12]	0.790
$31_{11,21}-30_{11,20}$	276378.367	27.1	346.5	276378.9	0.462	1.65
$31_{11,20}-30_{11,19}$	276378.367	27.1	346.5	[1]		
$31_{10,22}-30_{10,21}$	276380.286	27.8	323.2	[1]		
$31_{10,21}-30_{10,20}$	276380.286	27.8	323.2	[1]		
$31_{7,25}-30_{7,24}$	276617.294	29.4	266.7	276616.8	0.703	1.26
$31_{7,24}-30_{7,23}$	276617.868	29.4	266.7	[1]		
$31_{6,26}-30_{6,25}$	276856.499	29.8	252.4	276857.8	0.408[9]	0.672
$31_{5,27}-30_{5,26}$	277212.157	30.2	240.3	277211.4	0.233	0.708
$31_{4,28}-30_{4,27}$	277233.840	30.5	230.4	277232.7	0.500	0.738
$32_{2,31}-31_{2,30}$	279211.176	31.8	227.6	279210.2	0.502	0.790

[1] blended with the last one
[2] blended with $CH_3^{13}CH_2CN$
[3] blended with unidentified line
[4] blended with CH_2CHCN
[5] blended with HDO
[6] blended with CH_3CH_2CN b type
[7] blended with $CH_3CH_2^{13}CN$
[8] blended with CH_3OCOH
[9] blended with g$^-$-CH_3CH_2OH
[10] blended with $^{13}CH_3OH$
[11] blended with CH_3OCH_3
[12] blended with ^{34}SHD